EVN2015

THE FUTURE OF THE EUROPEAN VLBI NETWORK

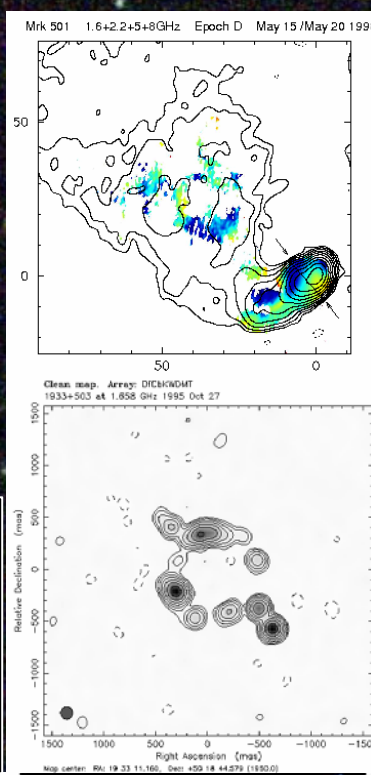

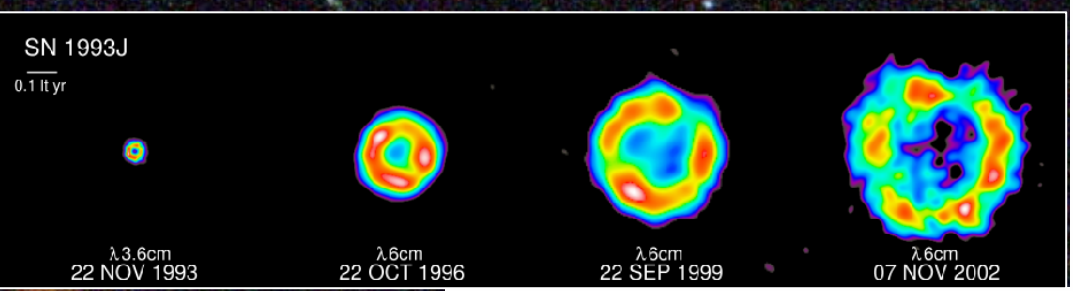

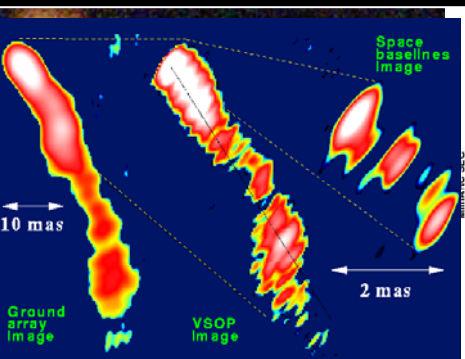

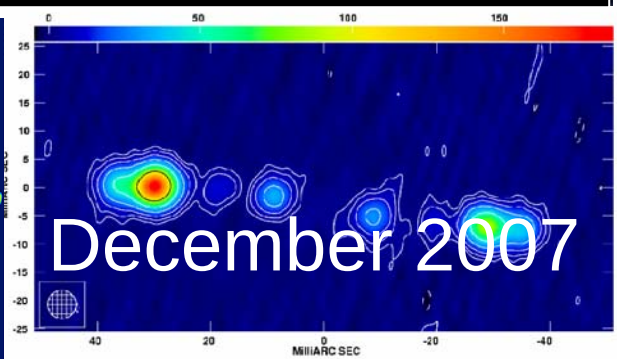

December 2007

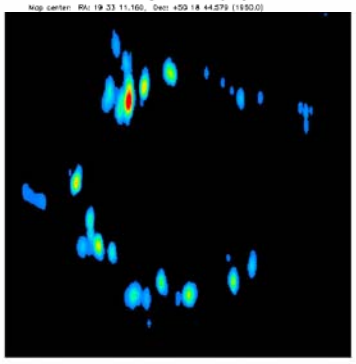

Dedication and Charge

This Vision document EVN2015 has been produced at the request of the Consortium Board of Directors of the European VLBI Network. A meeting on science applications for EVN2015 was held on 1-2 March, 2007 in Dwingeloo sponsored by ASTRON, JIVE and RadioNet.

Thanks are due to all persons contributing to this document.

With Contributions from:
Antxon Alberdi (IAA/CSIC, Granada)
Javier Alcolea (OAN, Madrid)
Willem Baan (ASTRON, Dwingeloo)
Anna Bartkiewicz (TRAO, Torun)
Robert Beswick (JBO, University of Manchester)
Marco Bondi (IRA, Bologna)
Gianfranco Brunetti (IRA, Bologna)
Andreas Brunthaler (MPIfR, Bonn)
Patrick Charlot (University of Bordeaux)
John Conway (OSO, Onsala)
Denise Gabuzda (University College Cork)
Simon Garrington (JBO, University of Manchester)
Hans-Rainer Kloöckner (Oxford Univ.)
Michael Kramer (JBO, University of Manchester)
Thomas Krichbaum (MPIfR, Bonn)
Andre Lobanov (MPIfR, Bonn)
Josep Martí (University of Jaén)
Raffaella Morganti (ASTRON, Dwingeloo)
Tom Muxlow (JBO, University of Manchester)
Zsolt Paragi (JIVE, Dwingeloo)
M.A. Pérez-Torres (IAA/CSIC, Granada)
Cormac Reynolds (JIVE, Dwingeloo)
Anita Richards (JBO, University of Manchester)
Ben Stappers (ASTRON, Dwingeloo; JBO, University of Manchester)
Olaf Wucknitz (JIVE, Dwingeloo; Universität Bonn)

Chapter Coordination:
Willem Baan (ASTRON), chapter B
Denise Gabuzda (University College Cork), chapter D
Simon Garrington (JBO, University of Manchester), chapter A
Anita Richards (JBO, University of Manchester), chapter C
Willem Baan (ASTRON), Zsolt Paragi & Cormac Reynolds (JIVE), technical sections

Final Coordination:
Willem Baan (ASTRON) & Zsolt Paragi (JIVE)

Executive Summary

The EVN mission is to enable discovery in radio astronomy through innovative VLBI instrumentation and the management of shared radio astronomy facilities within Europe and with affiliates in other countries.

This document describes the vision of the EVN for the period until the year 2015.

The first section presents the technical and operational possibilities that are available in 2007 or are to be available in the coming years for the development of the EVN.

The second section describes the four major areas of radio astronomical research that will be augmented or initiated using the capabilities of the EVN2015. The Science Cases are: *The History of the Universe*, *From Galaxies to Stars*, *From stars to Planets*, and *Cosmic Power Sources*. Within each of these Science Cases a large number of areas have been identified that depend on the increased capabilities of EVN2015.

The third section presents observational requirements from the Science Cases that are summarized and presented in terms of technical and operational requirements for the EVN2015.

The fourth section presents the recommendations to the EVN Consortium Board of Directors. These recommendations follow from the requirements for the Science Cases and present a route for the development of the EVN2015. The recommendations relate to: *Enhancing EVN Capabilities*, *Objectives for e-VLBI*, *EVN Correlation*, *User Services and Capabilities*, and *EVN Operations*.

The operational performance of the European VLBI Network depends on the effective collaboration of national observatories, the large collecting areas available at those observatories, and its success in incorporating the advances in technology. Target-of-opportunity capability and e-VLBI operation will contribute to robust and flexible operational procedures. Seamless EVN-MERLIN integration as the short baseline core of EVN can be achieved by adding EVN antennas to MERLIN and connecting the e-Merlin telescopes into the EVN correlator at JIVE. The increased correlation capability at JIVE of up to 256 Gb/s per radio telescope for routine operations with 32 stations will facilitate innovative research with EVN2015. Moreover, The increased operational bandwidths of 500 MHz at L-band and up to 1 GHz at C-band and the addition of new antennas with complementary frequency coverage and frequency capabilities will further increase the array sensitivity. The expansion of EVN at both low and high frequencies from 30 to 86 GHz represents a frontier of VLBI that will remain unique.

Table of contents

Executive Summary 3

Technical Potentials
1. The telescopes 5
2. The correlator 6
3. The logistics 6
4. The post-processing 6

Science Case A - The History of the Universe
5. The history of star-formation 7
6. The co-evolution of galaxies and AGN 9
7. Gravitational lensing 10

Science Case B - From Galaxies to Stars
8. Low Luminosity AGN and galactic black holes 15
9. Starburst galaxies and their constituents: near and far 17
10. The ISM in active nuclei 23
11. Celestial reference frames 27
12. The structure of the Milky Way 28

Science Case C - From Stars to Planets
13. The birth of stars and planets 31
14. Celestial recycling 34
15. Solar system science 39

Science Case D - Cosmic Power Sources
16. Accretion and outflows from relativistic objects 41
17. Unravelling the mysteries of microquasars 47
18. Stellar powerhouses 50

Technical Requirements
19. EVN system sensitivity 57
20. Frequency coverage and agility 57
21. Resolution, spacings and field of view 57
22. Correlator considerations 58
23. Flexible scheduling; rapid-response science 58
24. Calibration: amplitudes, phase stability & phase-referencing 59
25. Streamlining observing procedures and user tools 60
26. The EVN2015 requirements matrix 60
    Table 2 The EVN2015 requirement matrix 61

Recommendations to the EVN Board
27. Enhancing EVN capabilities 63
28. Objectives for e-VLBI 63
29. EVN correlation 64
30. User services and capabilities 64
31. EVN operations 64

Technical Potentials

The EVN has evolved significantly during recent years. The EVN is approaching a point where the back-end systems, the correlator, and the post-processing applications will limit the system capabilities and its potential. The introduction of the Mark5A disk-recording system has improved the data quality, extended the data recording rate to 1 Gbit/s, and opened up the possibility of real-time correlation (e-VLBI).

1 The telescopes

Technology will be available to extend the IF bandwidth of the EVN stations to 1 GHz in the L-band, and to 2-4 GHz in the C-band and higher. Full digital sampling of these IFs will be possible soon (dBBC project). Higher bit sampling (up to 8 bits) will enable RFI mitigation techniques, which are important when using the increased bandwidth. The long standing problem of frequency agility in the EVN will be partially solved by the increased bandwidth; however, rapid switching time between frequency bands on timescales of few seconds should be possible and must be pursued in order to carry out multi-frequency projects.

Connecting telescopes to the correlator real-time has already become a reality in the framework of the EXPReS project. Continuous monitoring of telescope performance during the experiments will be part of the standard observing mode and it will ensure robust operations. Rapid data analysis as well as on-the-fly changes in the observing schedule will be possible in response to the observational results. This technology will not only increase the flexibility of the array, but will make the EVN2015 highly competitive in a broader range of science applications.

This same technology could facilitate the transfer of calibration data from the telescopes to the correlator real-time, including accurate a-priori $T_{\rm sys}$ and instrumental phase calibration data (phase-cal detection and/or fast switching noise diode). There are various ways to improve on the phase-referencing capability of the array. Data from co-located WVR radiometers and GPS receivers could be used for the atmospheric and ionospheric phase calibration, respectively. These would be essential for astrometric applications, and especially for the rapidly developing mm-VLBI technique. An alternative method for phase-referencing could be the installation of dual-feed receivers on the smaller dishes. Even better, focal plane arrays would make it possible to observe several in-beam calibrator sources around the target, and to solve for the atmospheric and instrumental phase errors at the target position. Besides,this would improve the survey capabilities of EVN2015.

The EVN2015 sensitivity and imaging performance will be significantly improved with the higher bandwidths and with a number of new telescopes that will be built in strategic places (e.g. North Africa). Among the existing telescopes, the following are expected to become full EVN2015 members: Latvia (32m), Evpatoria (70m), Simeiz (22m), Miyun (50m), Kunming (40m), Yebes (40m), and the Sardinia telescope (64m). Additional telescopes are planned in Ireland, Madeira, the phase-1 SKA (Southern hemisphere), while SKA pathfinders (both hemispheres) and the 500-m FAST will come on line. This full array will be a powerful survey instrument enabling high-sensitivity snapshot observations of the sub-mJy radio sky before the full SKA will be operational.

2 The correlator

The rapid expansion of the array capabilities and the increase in data rates necessitates a new EVN Correlator. This correlator should be able to process data from 32 stations in real-time, handling up to 16 Gsamples per second at 8-bit sampling. This would lead to a data rate of up to 128 Gbit/s per telescope, or 4 GHz per bandwidth in both polarizations. Spectral line experiments should allow 16000 channels per correlation product with floating point accuracy, without sacrificing the continuum sensitivity. These capabilities facilitate mapping the full primary beam of a 25-m antenna in standard operations. Pulsar gating would enable the study of these highly relativistic systems at milliarcsecond resolution due to its great collecting area.

3 The logistics

The importance of rapid feedback and flexible scheduling as well as more dedicated time for VLBI observations is expected to increase significantly in the coming years. SKA pathfinders will discover a great number of new transients which will attract great attention from the scientific community. The real-time e-VLBI mode and dynamic scheduling capability of the EVN2015 would be ideally suited for such studies. It is expected that, using e-VLBI observing with ad-hoc global arrays including telescopes with various backend systems will be straightforward. The proposal mechanism (EVN/global Target of Opportunity requests) must be kept well aligned with these developments.

4 Post-processing

The increased data volume and the requirement of an easy-to-use VLBI array for researchers outside the field makes necessary the employment of a robust and reliable pipeline, which will provide maps as well as calibrated data. The EVN data archive should store calibrated data, with smart selection for data-mining. The user will be able to select the required field of view and resolution (spatial frequencies). Virtual Observatory tools will help provide effortlessly data products, such as light curves, spectra, pulsar time series, or overlays of images with results from other instruments.

Science Case A
The History of the Universe

5 The history of star-formation

One of the most enduring questions regarding the evolution of our Universe is how the level of star-formation has changed throughout the course of cosmic history. Star-formation rates within galaxies can be traced over a large range of wavelengths through both continuum, for example at ultra-violet and infrared wavelengths, and line emission such as Hα. However, in the cases of many of these tracers, the dust obscuration which is so prevalent in the most massive star-forming galaxies often results in reduced estimates of the star-formation rate. In addition, at high redshifts line tracers such as Hα, are transformed to parts of the electromagnetic spectrum that are not easily observed with ground-based telescopes. A recent estimate of the evolution of cosmic star-formation rate density from Hopkins & Beacom (2006) is shown in Figure 1.

Both thermal and non-thermal radio emission can be related crucially to the ongoing star-formation in galaxies at all redshifts, and offer a unique un-obscured tracer of the current star-formation. This relationship is underlined by the observed correlation between the radio and infrared emissions, both of which are related to star-formation; the infrared emission is produced from dust heated by photons from young stars, whilst the radio emission arises from synchrotron radiation produced by the acceleration of charged particles from supernova explosions. The study of such distant star-forming galaxies in the radio requires both the high-sensitivity and the significantly sub-arcsecond angular resolution of the EVN2015 to characterize the nature of such systems.

Deep radio surveys of the sky using newly upgraded instruments such as the EVLA and e-MERLIN will be able to detect thousands of faint, star-forming galaxies up to redshifts of a few. This will for the first time allow a definitive radio-based, and hence obscuration-free, census of the star-formation rate history of the Universe. Recent state-of-the-art deep field observations (e.g. MERLIN+VLA observations of the HDF-N by Muxlow et al. 2005) have shown that at radio flux density levels of <100μJy more than 70% of the sources are predominantly powered by star-formation and have angular sizes of between 1-2 arcseconds (see Fig. 2). At even lower flux densities the proportion of star-forming galaxies increases still further. Statistical stacking of current deep field radio data at the positions of many hundreds of infrared detected star-forming galaxies has already allowed these extremely faint starburst galaxies to be detected in the radio band and their size distribution investigated (see Fig. 3). In addition, such studies have extended the observed radio-infrared correlation to cover over six orders of magnitude in luminosity (see Fig. 4; Beswick et al. 2007).

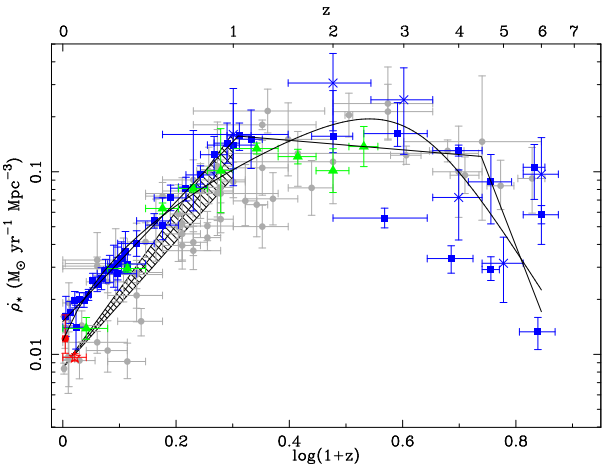

Figure 1: Evolution of Star-formation rate density with redshift (Fig. 1; Hopkins & Beacom 2006)

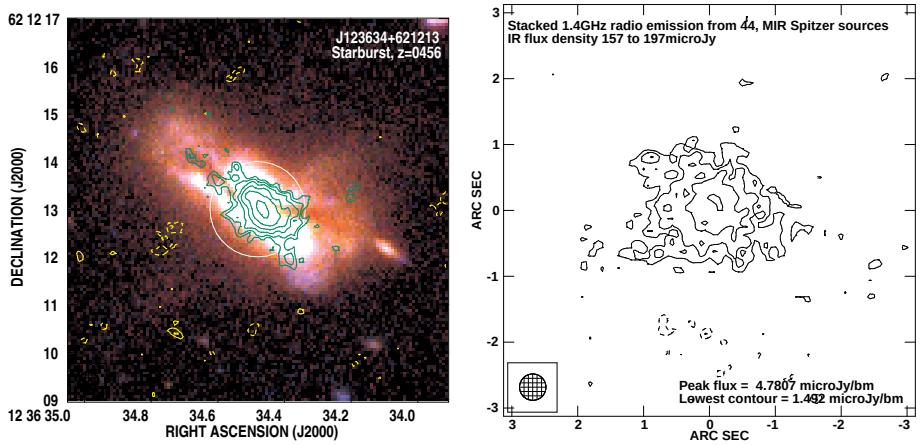

Figure 2: 1.4 GHz MERLIN+VLA contours overlaid upon a pseudo-real colour HST image of a starburst galaxy in the GOODS North field at a redshift of 0.456. CI=10μJy/bm)

Figure 3: Stacked 1.4 GHz radio emission from 44 MIR Spitzer sources with IR flux densities in the range 157 - 197 μJy. Radio CI=1.5μJy/beam

In many galaxies, both nearby and distant, strong current star-formation and an Active Galactic Nuclei (AGN) co-exist. The presence of an AGN, and any associated jet, can act to not only quench, via feedback, any ongoing star-formation but also to trigger regions of new star-formation as the jet interacts with the interstellar medium in the surrounding galaxy. In order to successfully separate the radio emission associated with AGN activity from that derived from star-formation in the distant Universe both high angular resolution and surface brightness sensitivity will be essential.

Lower resolution radio interferometers, such as the EVLA and e-MERLIN, will be the natural instruments to detect and measure the sizes of the radio emitting regions in this distant population of star-forming galaxies. e-MERLIN + EVLA at 4−6GHz will be used to image many hundreds of such systems to flux densities of a few tens of μJy in a single field. However, it is vital to separate and relate any AGN component from the starburst emission. Such embedded AGN may be radio quiet but still play an important role in controlling the star-formation process. EVN2015 will be in a unique position to make a detailed decomposition of the various emission pro-

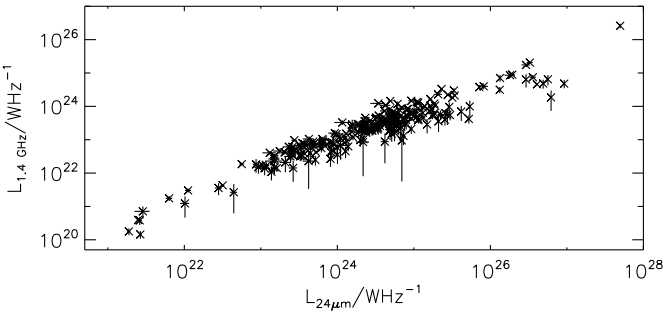

Figure 4: Observed correlation between 1.4 GHz luminosity and infrared 24 μm luminosity for 224 24 μm Spitzer sources with measured redshifts and significant radio flux density in the GOODS North field. The correlation extends over nearly 7 orders of magnitude in 24 μm luminosity. (Beswick et al. 2007)

cesses underway in distant galaxies. In particular the EVN2015 will be the instrument of choice when characterising the AGN contribution to the radio emission from distant star-forming galaxies by identifying radio cores (which may be faint but compact) and any associated jets, and separating these from the extended regions of star-formation.

A recent example of a very high angular resolution investigation of the AGN-Starburst connection has recently been performed with the EVN and Global VLBI at 1.4 GHz on a very distant (z=4.424) star-forming galaxy, J123642+621331, in the GOODS North field (Garrett et al. 2001; Chi et al. 2007). The majority of the radio emission is identified with an extended region of star-formation. However, the initial MERLIN+VLA image of this galaxy detected an additional compact component. VLBI imaging reveals a resolved jet-like extension running from the core through the star-forming region. This is thought to be one of the first examples detected of a high-redshift ULIRG in which the AGN jet activity is triggering and supporting the observed high star-formation rate and efficiency (see Figure 5; Chi et al. 2007).

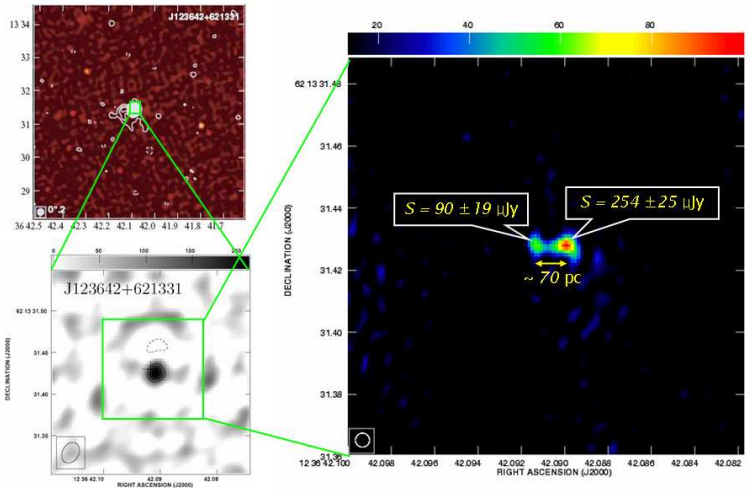

Figure 5: VLA J123642+621331 provides a first example of a high-redshift ULIRG where the AGN jet activity triggers and sustains star-formation with a high rate and efficiency. From Chi et al. (2007)

EVN2015 is likely to detect compact components in around 10% of such very weak μJy radio sources and deep integrations will thus yield several hundred detections in a single 10 arcminute field. The extreme angular resolution of VLBI combined with the superb sensitivity from the large telescopes included in EVN2015 will be vital in understanding the role of AGNs in the star-formation processes seen in such distant galaxies. It will also locate and survey the presence of radio-quiet AGNs, extending the completeness of our AGN census and constraining the models of the co-evolution of AGNs in their host galaxies.

6 The co-evolution of galaxies and AGN

The ubiquity of massive black holes in present day early type galaxies and the tight correlation between the mass of the black hole and the mass of the galaxy spheroid imply a close relationship in the evolution of black holes and their host galaxies. Active Galactic Nuclei are now widely regarded as the key to the feedback mechanism, which quenches the star-formation rate in massive galaxies as these galaxies reach a certain mass during the hierarchical build-up process. Different modes of feedback have been proposed, including Compton heating via X-ray emission from the AGN and the dynamic effects of radio jets emanating from the AGN. There is clearly a growing need for a complete census of AGN activity in order to trace how and when massive

black holes developed. However, it has become clear that in many wavebands, the majority of AGN activity is obscured and indeed the key phases of black hole growth are most likely to be associated with circumnuclear material providing strong obscuration. The quest to characterise this population of distant obscured quasars, which may outnumber the unobscured AGN by a factor of between 3 and 10, is one of the holy grails of current observational cosmology. So far, effort has concentrated on using deep X-ray and mid infra-red surveys. Recent work (e.g. Daddi et al 2007) using the 24 micron excess flux as an AGN indicator suggests that 25% of all galaxies at z=2 may harbour obscured AGNs. Observations at radio wavelengths offer, in principle, a powerful way to track down and investigate this population as well as the opportunity to study in detail the feedback modes involving radio jets. Arguably, there are no obscured radio AGNs but rather a minority population of radio loud AGNs and a population of radio quiet AGNs with flux densities of <10 μJy at z=2. Low-resolution radio observations can easily confuse radio emission from star-formation and AGNs; therefore, high-resolution observations are essential to isolate reliably the emission from AGNs. With μJy sensitivity and milliarcsecond resolution over a field diameter of several arcminutes, EVN2015 will be uniquely suited to the radio identification of radio quiet AGNs at $z > 1$.

7 Gravitational lensing

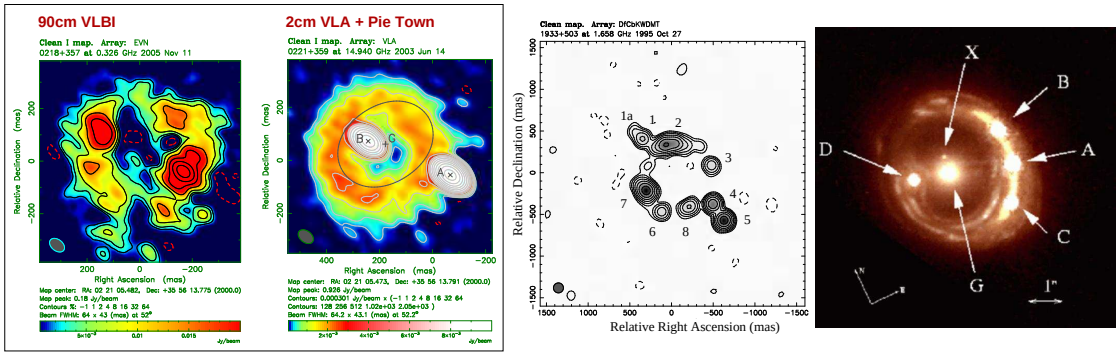

Figure 6: Left: The Einstein ring of B0218+357 with the VLA and VLBI. Low frequencies and/or high sensitivities are needed to map Einstein rings with VLBI. Centre: A ten-image radio lens (Sykes et al. 1998) that leads to accurate mass profile constraints. Right: A spectacular case of an optical lens. All these structures can be resolved with VLBI and provide information about mass models (Claeskens et al. 2006).

The VLBI applications of gravitational lensing are various. Part of the motivation for early lens studies was the idea of Refsdal (1964) to determine distances and thus determine the Hubble constant in one direct step, avoiding the uncertainties on all levels of the traditional distance ladder methods. This method needs two ingredients, the delay in light travel time between two lensed images, and a good model of the mass distribution of the lensing galaxy. The time-delay is used to define the scale of the lensing geometry, while the lens model defines all the angles that cannot be measured directly, such as the true source position. The lens model is used to produce one number which translates the time-delay into a value for the Hubble time ($1/H_0$). Radio astronomy (including VLBI) plays an essential role in lens studies and has produced some of the most reliable measurements (e.g. Biggs et al. 1999, 2003: Wucknitz, Biggs & Browne 2004).

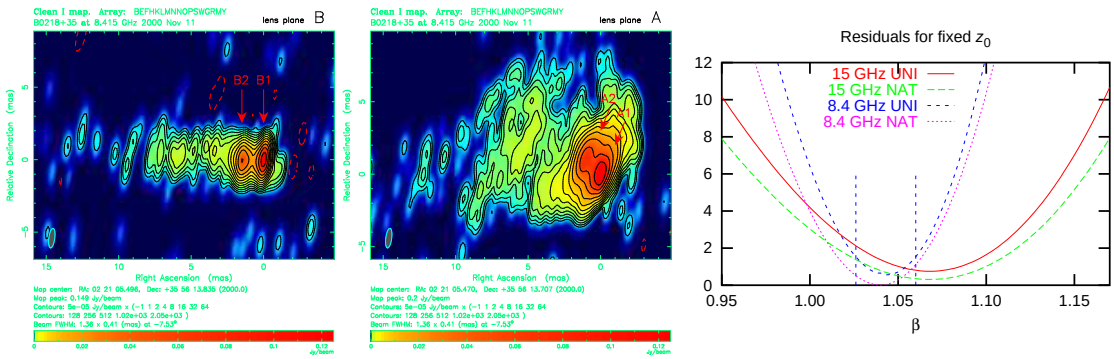

Figure 7: Left: Global VLBI maps (8.4 GHz) of the doubly imaged jet in B0218+357 (see Biggs et al. 2003). Right: Limits of the radial mass profile from such data (Wucknitz et al. 2004).

Even though independent measurements of H_0 are still an essential input to determine other cosmological parameters from CMB measurements, the main interest recently has shifted towards studying the lens galaxies themselves. Lensing is the only method that can provide accurate information about the mass distribution of high-redshift galaxies in order to allow for the study of their structure and evolution. Amongst the unsolved problems are the large-scale radial mass profiles, the central mass concentrations, and the amount of small-scale substructure that are expected from CDM structure formation simulations, but are not observed in the light distribution of galaxies.

Gravitational lensing probes the mass distributions in an unbiased way. Specifically tailored radio lens surveys like CLASS detect massive structures irrespectively of their visual appearance, even if they are completely dark. However, optical surveys are hampered by selection effects of bright lens galaxies and dust extinction in the lenses.

Information about the mass distribution is provided by the observed image configuration. Simultaneous mapmaking and modelling the lens mass distributions (LensClean method: Kochanek & Narayan 1992; Wucknitz 2004) greatly improves these results. For *pointlike* sources, this is limited to positions and flux densities of typically 2–4 images. For *resolved* but compact sources, relative magnification matrices provide additional information. Still, this information about the lensing potential and its derivatives is limited to a small number of positions. More valuable are lensed sources with many components (e.g. Fig. 6 centre) or lensed *extended* sources (e.g. the star-forming galaxy in Fig. 6 right), where components on different scales provide different constraints for the lens models.

7.1 Lensing with VLBI

VLBI is required to resolve compact radio sources in order to determine higher-order derivatives of the lensing potential which provide invaluable information about the global mass profiles of the lenses (e.g. Fig. 7). Currently the constraints for all well-studied lens systems strongly favour isothermal mass distributions ($\rho \propto r^{-2}$), but the sample is still too small for a final general statement.

For lensed sources with sufficient small-scale details, these can be used to study CDM substructure, which manifests itself in kinks or bends of radio jets on scales of milli-arcseconds (only resolvable with VLBI). These can be disentangled from the intrinsic source structure by having multiple images of the same source. Current evidence for substructure is mainly based on flux measurements which deviate from model-dependent expectations.

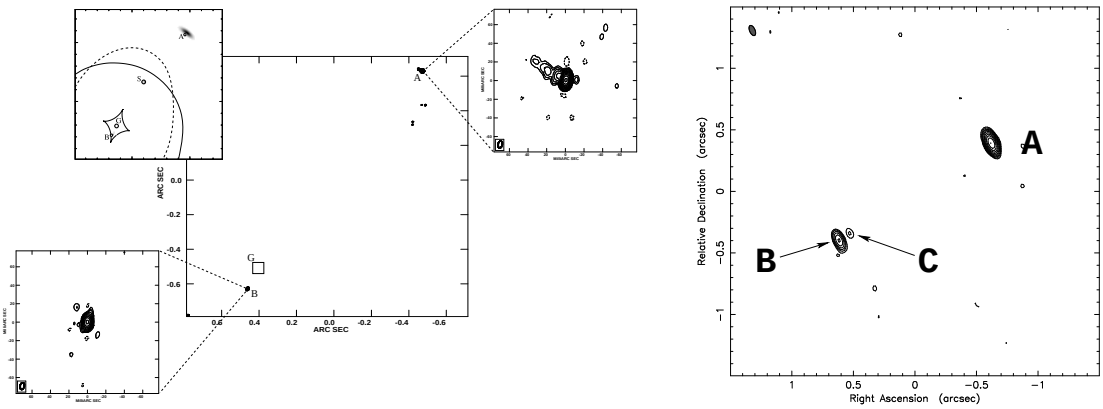

Figure 8: Left: VLBI (HSA) map of the double lens B1030+074. No central image was found at the expected position down to a flux density of 10^{-3} of the brighter image (see Zhang et al. 2007). This is not limited by thermal noise but by *uv* coverage and the hybrid-mapping stability. Right: J1632–0033 currently is the only lens system with good evidence for the detection of a central image (Winn et al. 2003). Improved sensitivity is required to find many more cases and decide between different models.

Observations of images close to the lens core are used to study the central mass concentrations (density cusps and supermassive black holes) with high accuracy. A steeper central mass profile would give a weaker central image. Flux density measurements or upper limits (see Fig. 8) provide information that cannot be obtained with any other method. This (as well as the substructure) is an area where the expectations depend on the properties of dark matter and where current observations seem to contradict the theoretical expectations. Lensing is the only way to study this topic at all distances, which is important for the study of the cosmic evolution.

An additional topic utilizing multiple imaging is the study of propagation effects like scattering or free-free absorption in the lens galaxy. Even though the intrinsic luminosity and spectrum are not known, the comparison of two images provides unambiguous information (e.g. Mittal et al. 2007).

As discussed above, lensed *extended* sources provide the optimal constraints for lens mass models. Since these sources typically have steep spectra, observations at low frequencies add invaluable information. In order to still reach the necessary resolution, the long baselines of VLBI are absolutely essential (see Fig. 6 left). The situation is more favorable at lower frequencies, where the resolution of the EVN is also better adapted to map structures on the scale of galaxies. In the near future, lens surveys with LOFAR will find many lensed extended sources, especially those with steep spectra.

References to Chapter A

Beswick, R., et al., 2007, in preparation
Biggs, A.D., Browne, I.W.A., Helbig, P., Koopmans, L.V.E., Wilkinson, P.N. & Perley, R.A., 1999, *MNRAS* 304, 349
Biggs, A.D., Wucknitz, O., Porcas, R.W., Browne, I.W.A., Jackson, N.J., Mao, S. & Wilkinson, P.N., 2003, *MNRAS* 338, 599

Claeskens, J.-F., Sluse, D., Riaud, P. & Surdej, J. 2006, *A&A* 451, 865
Daddi et al. 2007, astro-ph/0705.2832
Garrett, M.A., et al., 2001, *A&A*, 366, L5
Hopkins, A.M., 2004, *ApJ*, 615, 209
Hopkins, A.M., & Beacom, F.B., 2006, *AJ*, 651, 142
Kochanek, C.S. and Narayan, R., 1992, *ApJ* 401, 461
Le Floc'h, E., et al., 2005, *ApJ*, 632,169
Mittal, R., Porcas, R. & Wucknitz, O., 2007, *A&A* 465, 405
Muxlow, T.W.B., et al., 2005, *MNRAS*, 358, 1159
Perez-Gonzalez, P.G., et al.,2005, *ApJ*, 630, 82
Refsdal, S., 1964, *MNRAS* 128, 307
Seungyoup Chi, et al., 2007, *Proceedings 8th EVN Symposium.*
Sykes, C.M. et al., 1998, *MNRAS* 301, 310
Thompson, R.I., et al., 2006, *ApJ*, 647, 787
Winn, J.N., Rusin, D. & Kochanek, C.S., 2003, *ApJ* 587, 80
Wucknitz, O., 2004, *MNRAS* 349, 1
Wucknitz, O., Biggs, A.D. & Browne, I.W.A., 2004, *MNRAS* 349, 14
Zhang, M., Jackson, N., Porcas, R.W., & Browne, I.W.A., 2007, *MNRAS* 377, 1623

This page intentionally left blank

Science Case B
From Galaxies to Stars

8 Low-luminosity AGN and galactic black holes

8.1 Radio loud versus radio quiet AGNs

Radio cores and outflows/jets of radio plasma have been observed in many radio-quiet AGNs suggesting that all AGNs are radio emitting at some level. While the radio emission in AGNs is clearly associated to non-thermal process, the X-ray emission can be associated both to thermal (disk corona) and non-thermal (synchrotron IC jet) processes. The observed correlation between the X-ray and radio in low luminosity radio galaxies and in Seyfert galaxies is somewhat puzzling. While the X-ray and radio emission may correlate in low-luminosity radio galaxies because both are produced by a relativistic synchrotron jet, the same correlation (same slope but shifted towards lower radio luminosities) holds also for Seyfert galaxies, where the X-ray emission is thought to be produced by the accretion disk corona system (Figure 9 from Panessa et al. 2007). This suggests a common mechanism for producing the X-ray and radio emission in low-luminosity radio galaxies and in Seyferts or a combination of different mechanisms that produces the same spectral slope. The physical reason for this X-ray and radio correlation is unclear and needs to be investigated. It would be important to separate the radio emission of the core/jet (that can be associated to X-ray emission) from that of extended radio emission on larger scales or from compact starbursts (that may not produce any detectable X-rays). Moreover a detailed EVN2015 study of the radio jets, on the smaller scale, in a large sample of both low-luminosity radio galaxies and Seyferts could shed some light on the possible differences in the radio jet formation and propagation.

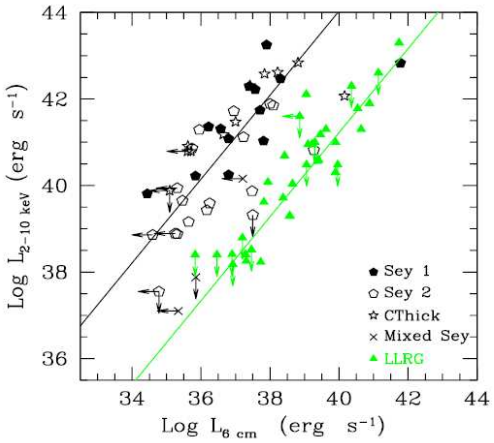

Figure 9: Hard X-ray luminosity versus 6 cm radio luminosity for a sample of galactic nuclei.

8.2 Aborted jets and radio quiet AGNs

Theoretical and observational efforts in understanding the physical reasons of the radio-quiet and radio-loud nature of AGNs are still failing to address this important issue. An increasing number of radio-quiet AGNs is found to be radio-emitting at some level and with a faint radio jet at small scales (aborted jets).

These jets are aborted because either their confinement (hydro plus MHD) is not efficient, or they have no continuous supply of energy from the BH, or they are radiatively inefficient, i.e. they are pair-jets made only by leptons that probably cool too fast due to IC scattering off external photons. In all these cases, a detailed study of the morphology of the aborted jets in radio-quiet AGNs is crucial to constrain possible scenarios. In the first case the polarization

properties of aborted jets at small scales should be radically different from those of standard jets. In the second and third case, multi-frequency spectra of the jets may identify the signature of particle cooling. The last case deserves much attention with theoretical investigations and the polarization (e.g. circular) properties.

The EVN2015 provides the required high-resolution, multi-frequency capability, and the ability to do the polarization studies.

8.3 Dynamics and structure of radio hot spots

When the head of a powerful jet interacts with the ISM/ICM, it forms a strong shock which may accelerate high energy particles. This is proved by the morphology and polarization properties of the hot spots, by means of optical and X-ray studies and also by theoretical modelling. Numerical simulations and some observations suggest that things may be more complicated, because the kinetic energy of the jets could be dissipated also via plasma instability and by the drilling of the jets into the ISM/ICM.

In this second case, the structure of radio hot spots is expected to be very clumpy and the polarization properties on small (10-100 pc) scales are expected to be very complicated. The compactness of these subcomponents allow a prompt detection with a "large effective area EVN" and also a production of IC emission. Finally the spectrum of the emitting electrons in radio hot spots is not always found to be in agreement with the expectations from the standard "diffusive shock" acceleration model, and in some cases the spectrum is too steep or too flat. This is expected in the case that several populations of radio emitting particles are accelerated (or re-accelerated) in different regions of the hot spots and coexist in the hot spot volume. Clearly high-resolution spectra of different clumps in the hot spots combined with high-resolution optical follow-up will greatly contribute in addressing this issue.

This research requires the high-resolution, high-frequency, and polarization capabilities of the EVN2015.

8.4 GLAST and EVN

GLAST will provide a number of gamma ray sources which are a factor of 30 larger than those detected by EGRET. The link between the gamma ray and the radio emission is well known and these sources will be (and indeed have already been) the target of a monitoring campaign by the VLBA. Based on the radio-gamma ray correlation, more that 1000 sources have already been selected and observed by the VIPS program (VLBA Imaging Polarimetry Survey). These are the sources that will be detected during a gamma ray flare by GLAST, and they will be monitored at different frequencies with VLBA during a gamma ray flare. The e-VLBI capability of the EVN2015 will provide competitive multi-frequency high-fidelity imaging of these sources.

8.5 The first BHs and their connection with starbursts

An important issue in the study of high redshift IRX sources and of the starburst-AGN connection is the growth of the first BHs and how they become active. Deep multi-frequency surveys have discovered luminous X-ray and IR sources at high redshift, which are usually followed up by "low" (arcsec) resolution radio observations. Potentially the first starburst activity might trigger the start of the fuelling of the central AGN and, vice-versa, the AGN activity could affect the starburst around the AGN itself. Deep high-resolution multi-frequency EVN2015 observations will reveal the presence of weak AGNs and allow the study of the starburst-AGN connection.

9 Starburst galaxies and their constituents: near and far

The star-formation process is responsible for the majority of observed activity in the Universe with all galaxies, at some point in their lifetime, undergoing a starburst phase; consequently, understanding starburst galaxies is crucial to many areas of astrophysics. It has direct implications for cosmology, galaxy formation and evolution, massive star-formation, and probes the physical processes underway in the interstellar media (ISM) in extreme environments. Whilst extragalactic star-formation is widely studied at all wavelengths, radio astronomy occupies a unique and important position. Radio waves trace physical conditions that are different from those probed by optical and infrared wavelengths and provide the highest angular resolution images available. Crucially, they are also unaffected by dust obscuration allowing the dust enshrouded centres of galaxies to be penetrated.

With respect to the study of star-formation in nearby galaxies, the EVN already occupies an important niche as a high-resolution, high-sensitivity radio instrument. Each individual starburst galaxy provides a laboratory of rapidly evolving stars, enshrouded by gas and dust, all at essentially the same distance. The high angular resolution and sensitivity of VLBI is ideally suited for detailed studies of these objects. Such observations uniquely probe the physics of supernovae, masers, HII regions and the cool ISM at the highest angular resolution. The current capabilities of VLBI networks make possible the investigation of the details of star-formation processes in individual starbursts in galaxies. However, the network's current capabilities limit the extent of this research. Primarily the brightness sensitivities obtainable by VLBI observations allow only the nearest and brightest objects to be studied. The inherent sparseness of u-v coverage of VLBI arrays limits the fidelity of the images of faint evolving sources, such as supernova remnants.

Currently radio astronomy is at the dawn of a sensitivity-revolution arising from the exploitation of new technologies and the construction of more powerful radio telescopes, such as ALMA, the EVLA, e-MERLIN and LOFAR. Future upgrades of the EVN2015 will provide an integral part of this innovative suite of radio instruments available to researchers over the next decade.

9.1 Understanding starburst galaxies - Fundamental questions

At low redshifts each individual starburst galaxy provides a unique opportunity to study star-formation in an extreme environment. It is a laboratory containing rapidly evolving stars, HII regions, supernovae and their remnants, all of which are enshrouded by gas and dust and are located at essentially the same distance. The majority of these systems are found to be undergoing galaxy-galaxy interactions or mergers, representing many different stages of galaxy evolution, and provide a wide range of environments where star-formation can be investigated.

At the highest redshifts, where the detailed parts of individual starburst systems cannot be fully resolved, they can be used to measure both the rate of star-formation and the positions of the centres of such activity within these distant galaxies. The physical processes taking place in both nearby and distant systems may be considered as equivalent, and it is thus essential to study both in order to draw parallels and to address the wider cosmological context.

Extremely sensitive high-resolution radio studies of both nearby and distant starburst galaxies will expand our understanding, and in-turn provide strong constraints on the star-formation history of the Universe.

The outstanding questions regarding starburst galaxies can be separated into two distinct but interrelated areas: a) the causes of the extreme star-formation and b) the consequences of this star-formation. High-resolution radio observations with the EVN2015 will reward our efforts in each of these areas.

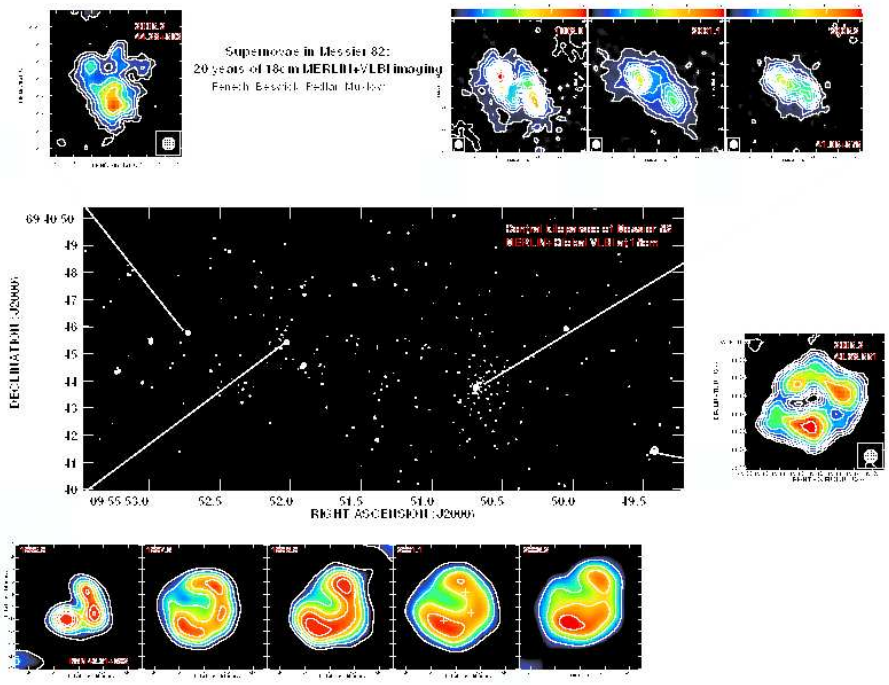

Figure 10: 20 years radio monitoring of the supernovae in M 82 at 18 cm. Central image shows a deep, combined MERLIN plus Global VLBI image of M 82. Inset images show the power of VLBI arrays to image the structures of individual supernova remnants and over time measure their evolution. Prior to the enhanced brightness temperature sensitivity of these latest 2005.2 combined MERLIN and VLBI data, only a few individual supernovae could be detected in M 82 and imaged at mas resolution with VLBI. The combined data has increased, by an order of magnitude, the number of sources that can be studied on sub-parsec scales (Beswick et al. 2006; Fenech et al 2007)

9.1.1 The causes of extreme star-formation

In order for the extreme levels of star-formation in starburst galaxies to occur, certain physical conditions are required. First and foremost there needs to be an abundance of material in the form of gas and dust from which stars can be formed. However, this material must exist within suitable ranges of densities and pressures so that it is conducive to the rapid formation of stars. Some of the perennial questions include how and from where is this material transported into the starburst region, and, consequently, how is the starburst triggered.

It is widely accepted that the vast majority of starburst galaxies, both at high and low redshifts, are associated with galaxy-galaxy mergers or interactions (Sanders et al. 1988) and that these merger events provide the material and create the conditions needed to form a starburst system. However, the detailed kinematics and composition of the gaseous material that *fuels* the starburst needs to be studied further at a suitably high angular resolution (preferably on sub-parsec scales).

The one method by which the cold neutral and the molecular gas within starburst galaxies can be currently probed is via spectral line absorption and maser observations at radio wave-

lengths. For example, neutral hydrogen (HI), which is one of the fundamental building blocks of stars, can be observed via the absorption of it's 21 cm transition against a more distant source of non-thermal radio emission. This technique uniquely allows the HI to be probed on milli-arcsecond scales. It should be noted that due to the brightness temperature of the 21 cm line of HI ($T_B \approx 100$ K) and the sensitivity limits of current and future radio interferometers, this line cannot be observed in emission with angular resolution finer than a few seconds of arc. Even in the era of the SKA, the EVN and other similar long-baseline radio interferometers will be the only instruments capable of extragalactic HI studies on angular scales better than 100 mas.

Thus the EVN provides an instrument that is capable of exploring the detailed cool neutral and molecular gas structure within the centres of nearby starburst galaxies on parsec and even sub-parsec scales (See Section 10). In the coming decade this capability will be complimented by new telescopes in other wavebands. In particular, ALMA studies of molecular line emissions at high angular resolution in starburst galaxies are well-matched with radio studies with the EVN2015.

9.1.2 The consequences of extreme star-formation

Starburst galaxies allow us to study the detailed processes of massive star-formation. After nearly two decades of studying the star-forming galaxies nearest to the Milky Way, our understanding is still in relative infancy. In order to extend the study to significantly fainter and more distant systems, a considerable increase in sensitivity and fidelity is required for high-resolution imaging. A few individual supernovae have been imaged from birth, but the evolution of such objects into remnants is critically dependent on their interaction with the surrounding ISM. Possibly not every supernova explosion produces a visible remnant.

High-fidelity, high-resolution imaging with the EVN2015 will be crucial in studying the detailed evolution of supernova remnants and their interaction with the surrounding ISM. The initial expansion velocities of many such systems can be measured directly and their slow-down with time. For the first time the high-fidelity EVN2015 radio images of the evolving remnant will be used to derive reliably the properties of the surrounding clumpy medium.

9.2 VLBI imaging M 82 and other nearby starbursts

Studies have been initiated to measure the expansion velocities and the deceleration of a few nearby compact remnants and to probe the nature of their environment, which is thought to be extremely clumpy. The interaction of the ejecta with the environment and the Sedov phase expansion probe the local ISM. There are indications that SN in environmental voids may produce no observable remnant. In M 82, the derived star-formation rate implies a SN rate of 1 every $\sim$12 years, compared to the observed SNR rate of 1 every $\sim$30 years.

The starburst regions of M 82 have also produced a population of transient source with lifetimes of t$<$6 months. The nature of these sources remains unknown and an understanding of these sources requires a statistical approach and the enlarging of the sample by at least an order of magnitude. Systematic studies will detect and resolve any recent radio transients (Fig. 10) .

9.3 Deep imaging using the EVN2015 with EVLA and e-MERLIN

The studies of the SNR in the nearby starburst M 82 need to be extended to older and fainter remnants. Similar SNR studies are also possible in the 30-some starburst galaxies within a distance d$<$30Mpc [SNR 50μJy, size 30mas] (Fig. 11). Enhancements to the EVN will allow similar studies of SNR to be undertaken in the several tens of starburst galaxies within a distance of 30 Mpc.

In particular, high-fidelity imaging and spatial frequency filtering will allow the extraction of faint remnants from any extended radio background. The angular resolution and multi-frequency coverage of VLBI will provide both the structural and spectral information required to separate cleanly the weak SNR and HII regions. These high-fidelity, multi-frequency imaging experiments will allow the study, for the first time, of the interstellar medium close to individual SNR on parsec scales via free-free absorption. Also the magnetic field strength in the medium can be deduced from the rotation measure of any linearly polarized emission detected in the SNR.

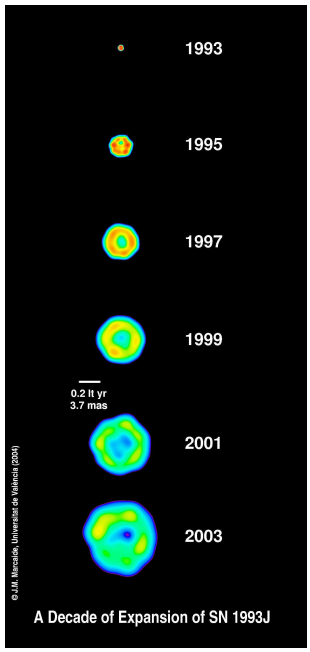

Figure 11: A decade of expansion of the radio supernova SN1993J in M81. SN1993J as one of the nearest radio supernovae has been imaged extensively with VLBI. Long-term monitoring experiments have measured the expansion of the radio emitting shock-wave and its deceleration due to its interaction with the surrounding CSM (from Martí-Vidal, Marcaide & Alberdi 2006).

9.4 Local late-stage GRB afterglows

M 82 hosts one particularly unusual source, 41.95+575. This radio sources is the most compact within M82 and differs significantly from the more typical shell or partial shell-like supernova remnants. Since high-resolution radio monitoring of M82 began, more than 40 years ago, this source has shown a constant decrease in flux density of 8.5 percent per year. In fact, in some of the earliest radio observation in the mid 1960s, the flux density from this one source was dominating the entire flux density of M82. On milliarcsecond scales, 41.9+575 exhibits an evolving bi-polar structure with a relatively slow expansion of $\sim$1500 km s^{-1}, which is situated at the centre of a large HII bubble with a radius of $\sim$100 light years. Making the crude assumption that the 41.9+575 has been and continues to be in free expansion, we can estimate a dynamical age of the source of around 100 years.

Considering 41.95+575's estimated dynamical age and observed flux density decrease, it would have been a spectacular radio source in its youth. However, the true nature of this source remains elusive. It has recently been speculated that this object may be a late-stage radio afterglow of a (non-aligned) Gamma-ray burst (GRB) at about 100 years after the outburst. The significantly improved imaging fidelity of the enhanced EVN2015 will be required to verify this interpretation. Furthermore, this object is only 3 Mpc away, which raises the question as to how many more of these objects will be observable within distances of a few tens of Mpc. Again the enhanced EVN will be the crucial instrument in both the discovery and the interpretation of these objects. With an age of about 100 years, objects such as 41.95+575, if they are indeed late-stage radio afterglows of GRBs, can only be studied locally and with the linear resolutions of many orders of magnitude greater than their younger, high redshift counterparts (Muxlow et al. 2005).

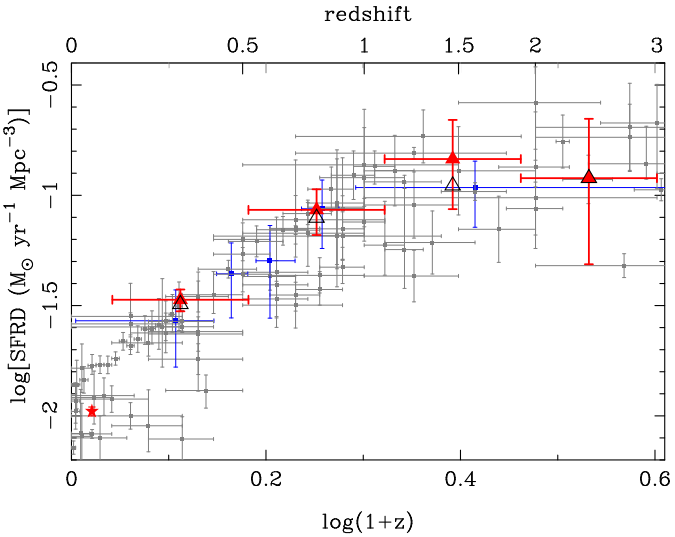

Figure 12: The co-moving star-formation rate density (SFRD) as a function of redshift from current radio surveys (from Seymour et al. 2007). Most surveys, both radio and at other wavebands, agree that the rate of star-formation increases with redshift up to at least $z \sim 1$. Beyond this point data becomes sparse; however, observations are now beginning to confirm the flattening of the SFRD beyond this point. Future radio observations will constrain this further.

9.5 Star-formation at high redshift

By calibrating our understanding of the star-formation process in nearby starburst galaxies, it is possible to derive reliable star-formation rate indicators. Deep radio surveys of the faintest radio sources at centimetre wavelengths have shown that below $\sim$100μJy the population becomes dominated by distant star-forming galaxies. Radio luminosities (together with the far-IR) have been shown to be one of the best extinction-free measures of star-formation rates. The established IR-radio correlation now extends to > 7 orders of magnitude in luminosity, allowing us to probe how the star-formation density varies with cosmic epoch (Figure 12).

It is thought that AGN activity via feedback is very important in controlling star-formation. Most distant starburst galaxies show no evidence of significant AGN activity, however some very luminous high redshift systems appear to contain embedded AGNs. Others emit hard X-rays indicating an active AGN but no compact radio source is as yet detected. Deep e-MERLIN plus EVN images will probe for embedded AGNs in such systems (Fig. 13).

9.6 Star-formation history from starburst luminosities

For those weak sources which we can at present only study statistically, e-MERLIN, EVLA and enhanced EVN should image >1000 individual starburst systems to 4μJy at 1.4GHz with perhaps 150-200 at high redshift in a single field. Many thousands of systems with radio flux densities <1μJy will be studied statistically. Many sub-mm starburst systems at high redshift show evidence for substantial AGN activity. The enhanced EVN will play a pivotal role in probing the role of AGNs in such systems and estimating the AGN contamination of the radio emission by the starburst. It will investigate the role of feedback and jet-induced star-formation and ultimately help derive the star-formation rate history of the Universe.

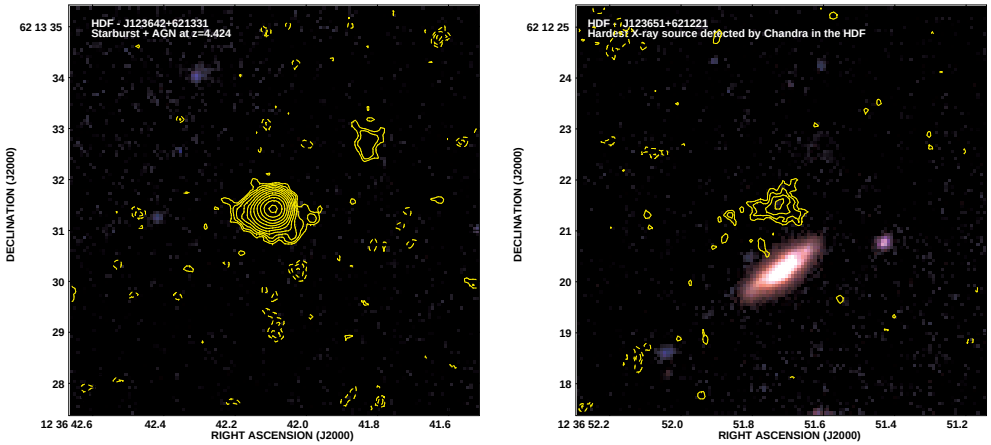

Figure 13: Deep MERLIN plus VLA imaging of the Hubble Deep Field North. The images (contours multiples of 10μJy bm^{-1}) show the 1.4 GHz radio emission overlaid upon a deep pseudo-real colour HST ACS imaging. The images show two optically faint, high redshift radio sources. In the radio both sources show characteristics of star-forming galaxies; however, high-resolution imaging of J123642+621331 (left) using the EVN (also see Figure 5) shows an embedded AGN in this redshift 4 source (Muxlow et al 2005; Richards et al 2007).

10 The ISM in active nuclei

10.1 The evolution of gas structures in AGN and SBN

The Interstellar Medium (ISM) in the circum-nuclear regions of AGN and Starburst Nuclei (SBN) provides a unique probe of the physical conditions in these regions and of the ongoing physical processes, such as the way the energy released by the active nuclei feeds back to their surroundings (see e.g. Morganti et al. 2004). Studies of the ISM also probe the evolutionary stage of the galaxy by tracing the presence of gas at larger radii and answering questions on the (large) quantities of gas that may surround the galaxy as a result of the merger.

H I and OH can be observed in absorption against the central regions of radio-loud AGNs and SBNs with relatively strong radio cores, that reveal circumnuclear disks (with typical $\tau > 0.01$). Broad (~ 1000 km s^{-1}), blueshifted and very shallow ($\tau \lesssim 0.001$) absorption systems have been detected in H I and OH in a handful of sources (Morganti et al. 2005; Baan 2007). An example of a broad H I absorption line is found in the radio galaxy 3C 293 (Fig. 14). The observed terminal velocities of the wings in the lines of OH emitters and OH and H I absorbers vary with the intensity of the activity of the nuclear region expressed as $L_{\rm FIR}$ (Fig. 15), such that a fraction of the energy generated gets converted into mechanical energy. In some galaxies these wings represent massive nuclear outflows (blow-outs). However, the broad blueshifted absorbers in AGNs do not fit this picture and may be related to jet-ISM interactions (see Fig. 15). While circum-nuclear structures are important in the context of the unified schemes, the outflow features may be the signature of feedback due to the AGN and SBN activity. This feedback is considered an important element in galaxy evolution as it can, by clearing the circum-nuclear regions from gas, quench star-formation and limit the growth of the super-massive black hole. Understanding the evolution with redshift of these processes will be of crucial importance.

The neutral atomic (H I) and molecular (OH) component of this medium can be readily studied at the radio wavelengths covered by the EVN2015. The capabilities for frequencies down to 300 MHz will make it possible to study these lines (H I and OH) in absorption in objects up to redshift $\sim$ 3. The combination of a large instantaneous bandwidth and wide-field imaging will allow the exploration of large volumes via "blind" surveys and the study of the nuclear regions of SBN and AGN in a statistically significant manner. The ISM in different classes of enshrouded SBN and AGN at different epochs will show whether the characteristics of the circum-nuclear gas change with redshift and whether the radio properties relate to differences in the ISM in which they are embedded.

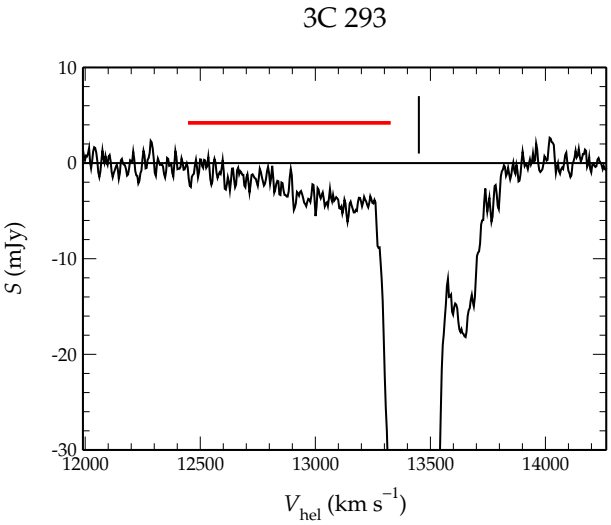

Figure 14: Example of broad blueshifted H I absorption detected against the central regions of the radio galaxy 3C 293. The horizontal line indicates the extent ($\sim$ 1500 km s^{-1}) of the blueshifted wing of the H I absorption. From Morganti et al. (2005).

OH and H I absorption of $\tau \sim 0.01$ or larger, typically found associated with the circum-nuclear disks, can at present be detected in sources of at least 100 mJy flux density. Broad and shallow ($\tau \lesssim 0.001$) absorption systems will be detectable in sources of$\sim$ 200 mJy and again up to high redshift. Only increased sensitivity of the EVN2015 above 1 GHz and particularly below 1 GHz will result in increased detection rates (number per square degree) absorption in radio emitting AGN and SBN. The study of the nuclear ISM can be done with pointed observations on known radio sources or with "blind" searches (both for H I and OH). These searches can be centered on well-studied fields in order to exploit the complementarity with other data (e.g. deep optical observations or multi-object spectrograph data). A broad instantaneous bandwidth of at least 250 MHz (at z = 0) or selectivity over this range will allow the exploration of large volumes of both H I and OH and of extremely broad lines. Blind searches with a large bandwidth for SBN and AGN will simultaneously provide deep continuum surveys and information about spectral index and rotation measure (RM) of the detected objects.

10.2 The megamaser perspective

Megamaser (MM) emission traces the nuclear regions of different populations of active galaxies. In AGN the H_2O MM emission comes from parsec scale accretion disks around super-massive black holes and from interaction regions between jets and the ambient medium. Kilomaser H_2O emission has also been seen in star-formation regions in nearby galaxies. The OH MM emission originates in (Ultra-)Luminous Infrared Galaxies, (U)LIRGs, that are powered by an intense nuclear starburst or by a nuclear hybrid with a super-massive black hole surrounded by a star-forming environment. The powerful molecular emission results from amplification of the embedded radio continuum by excited (pumped) foreground gas.

10.2.1 OH and H_2CO megamasers

The OH megamaser (OH MM) emission originates in the nuclear ISM and the molecular torus structures surrounding the star-forming nuclear region (Fig. 16). High-brightness components resulting from shocked (edge-on) shells and dense cloud superpositions and diffuse components tracing the star-forming ISM and the gas in a torus have been found in these sources (see Fig. 16). Current observational data with the EVN network detect increasingly higher gain components and miss 50% or more of their flux as compared with low-resolution data (Rovilos et al. 2003, 2005; Baan et al. 2008). The OH MM provide a unique probe of the dynamically active star-forming nucleus where molecular structures with varying densities are intermingled with massive stars and shocked layers of gas due to supernovae and their remnants.

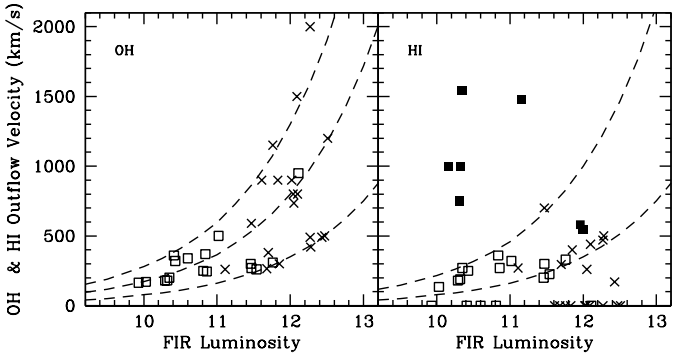

Figure 15: Maximum OH and HI outflow velocity observed for the sample of known absorbers and OH megamasers. Crosses represent megamaser sources with OH emission and H I absorption and open squares represent sources with HI and OH absorption. The filled square are HI absorbers in powerful radio galaxies taken from Morganti et al. (2005). The dashed lines represent the energy-conserving $L_{\rm FIR} \propto V^3$ curves for the terminal velocity of the nuclear outflows where the vertical scale varies with the displaced ambient column density. From Baan (2007).

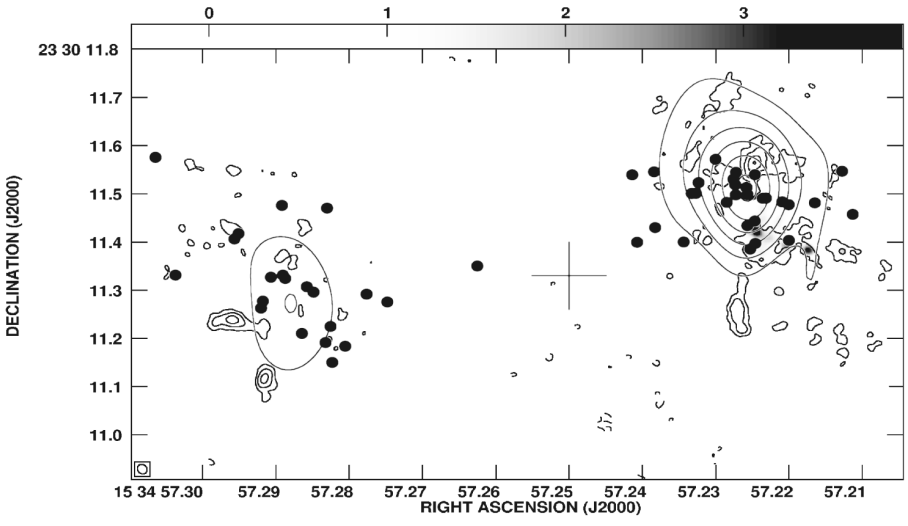

Figure 16: The OH emission at the two nuclei of Arp 220. The high-resolution EVN map of the 1667 MHz emission from Rovilos et al.(2003) has been overlayed with the map of supernovae in the two nuclei from Parra et al. (2007). Continuum contours indicate the location of the radio nuclei. The superposition is a best effort (0.1" = 35 pc). From Baan (2008).

The nucleus of the nearby OH and H_2CO MM prototype Arp 220 displays supernovae and SNR as point sources at both starbursting nuclei (Parra et al. 2007). Line emissions at 1665 and 1667 MHz in the molecular gas originate in the ISM in front of these SNRs. Large scale outflows have been also observed in the 1667 MHz line in Arp 220 and a number of other OH MM (Baan, Haschick & Henkel 1989; Baan 2007). The FIR radiation field is the primary pumping agent for the OH in the nuclear regions, while for H_2CO both collisions and the FIR radiation field may provide the pumping. Formaldehyde emission also results from amplification but the currently known lines are (still) too weak to be observed with VLBI, although successful MERLIN and VLA-A observations have been done.

The OH MMs are the signposts of the ULIRG population and Gigamasers (GM) are found among the most luminous sources. ULIRGs trace the galaxy merger history of the universe with redshift. The merger rate peaks at redshifts of about 2 - 3 where the massive galaxies in the present universe are formed. OH MM and GM are detectable out to such redshifts and already the (currently) two most distant ULIRG/OH GM were mapped at a redshift of 0.26 (at 1316 MHz) (Baan et al. 1992, Darling & Giovanelli 2001, Philström et al. 2004). While most of the ULIRG energy may result from massive star-formation, a fraction of the sources exhibit circum-nuclear star-formation in AGN sources. An example of such a source is Mrk 231 where the OH MM emission originates in a molecular structure surrounding the AGN (Fig. 17).

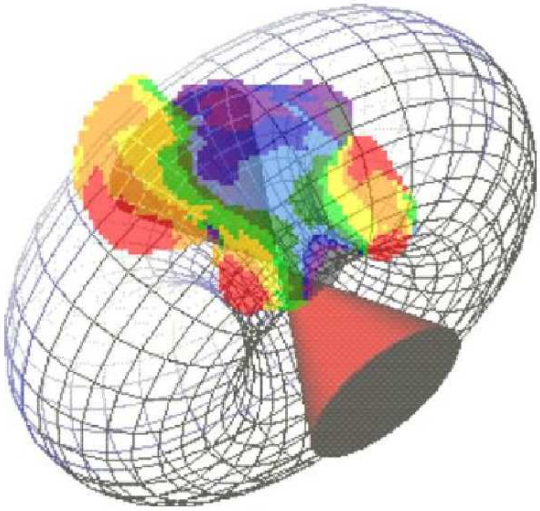

Figure 17: The velocity field of the OH MM emission at the nucleus of Mrk231. The velocity field indicates rotation of the masering gas that has been modelled to be part of a thick torus of molecular gas and dust (indicated by the grid model) surrounding the starburst-AGN hybrid nuclear region. The cones indicate the two jets that emerge from the nuclear region feeding the extended radio structure. Mrk 231 is one of a few galaxies that have a clear AGN at their nucleus as most OH MM and ULIRGs are starburst powered. From Klöckner, Baan & Garrett (2005).

The EVN2015 spectral line sensitivity above 1 GHz and particularly below 1 GHz is the limiting factor for targeted and blind searches and for deep imaging of OH MM at high redshifts. The resolution of the EVN2015 allows imaging of an OH-MM nucleus with a size of 100 pc with ten beams across the nuclear region out to z = 0.033 and with the Chinese, South African stations to z = 0.1 and with Arecibo and the VLBA to z = 0.17. Imaging could be done for redshift up to 0.6. A spectral bandwidth of 250 MHz or selectivity covering that range would allow simultaneous observations of OH and H I. The characteristics of OH MM complement the high-sensitivity molecular studies of active nuclei that will become feasible with ALMA.

10.2.2 H_2O-megamasers

H_2O MM are important signpost of AGN activity. A subset of these MM traces the central parsec scale accretion disk of the AGN and are found to be valuable cosmological laboratories. A significant sample of objects similar to the archetypal warped Keplerian disk in NGC 4258 (e.g. Claussen et al. 1984; Nakai et al 1993; Haschick, Baan & Peng 1994; Herrnstein et al. 1999) may be discovered.

Direct mapping of nuclear disks may be used to study dark energy, make precise estimates of H_0 to anchor the extragalactic distance scale, and to probe the central structures of accretion disks around supermassive black holes. For unresolved nuclear disks, the velocity drifts and the rotation velocity will extend the distance scale, albeit with less precision, well into the Hubble flow. The most distant H_2O maser found to date is in quasar SDSS J0804+3607 at a distance of 2.4 Gps (Barvainis et al. 2005), which is good evidence that molecular gas exists at very early epochs.

Another important group of H_2O sources displays emission from shocked jet-ambient ISM interaction interfaces away from the AGN. A class of H_2O masers probes the interaction between radio jets and ambient molecular clouds, such as seen in NGC 1052 (Claussen et al. 1998) or Mrk 34 at a distance of 205 Mpc (Henkel et al 2005). A water megamaser has also been detected in the FR-II radio galaxy 3C 403, indicating disk accretion or jet interaction (Tarchi et al. 2003). These structures may be up to 100 pc from the AGN, much further out than nuclear disks. Some less powerful kilomaser sources trace the star-formation in some nearby galaxies. An example of the latter would be NGC 2146 (Tarchi et al. 2002), which shows that UCHII regions may be detected up to distances of 50 Mpc.

The water vapour is pumped collisionally in shocks or by the X-ray radiation field from the AGN or possibly even by the X-ray binaries in a starburst. The gains of the H_2O emission is relatively high such that most of the emission is recovered in VLBI experiments and there is little in low surface brightness components (Braatz et al. 2004; Henkel et al. 2005; Greenhill 2007). An H_2O-MM nuclear disk with a size of 3 pc can be mapped with ten beams across the region with the EVN2015 out to z = 0.015, if the China and RSA stations are included to z = 0.05 and with the VLBA to z = 0.06.

The EVN2015 would benefit from an increase of bandwidth for simultaneous line and continuum experiments. Increased collecting area for the EVN2015 improves imaging capabilities at a higher sensitivity. Broadband capabilities allows simultaneous observations of OH (all four lines) and H I while multi-epoch observations will help to understand the pumping mechanism in regions of 1-2 pc. Polarization measurements and Zeeman splitting are important for OH and H_2O MM, for the magnetic field close to the jet and for the nuclear magnetic field.

11 Celestial reference frames

The construction of a highly-accurate and stable celestial reference frame based on positions of extragalactic radio sources has been an important achievement of the VLBI technique during the past 20 years. This reference frame is the basis for various geophysical and astrophysical applications such as monitoring the Earth's orientation, measurements of plate tectonic motions, spacecraft navigation in the solar system, or phase-referenced observations of weak radio sources angularly close to the reference frame sources.

The International Celestial Reference Frame (ICRF), the current IAU-adopted fundamental frame (Ma et al. 1998, Fey et al. 2004), includes a total of 717 sources distributed over the entire sky with 250 μas position accuracy at best (Fig. 18); these positions were derived from repeated (multi-epoch) VLBI observations conducted between 1979 and 2002 with international geodetic

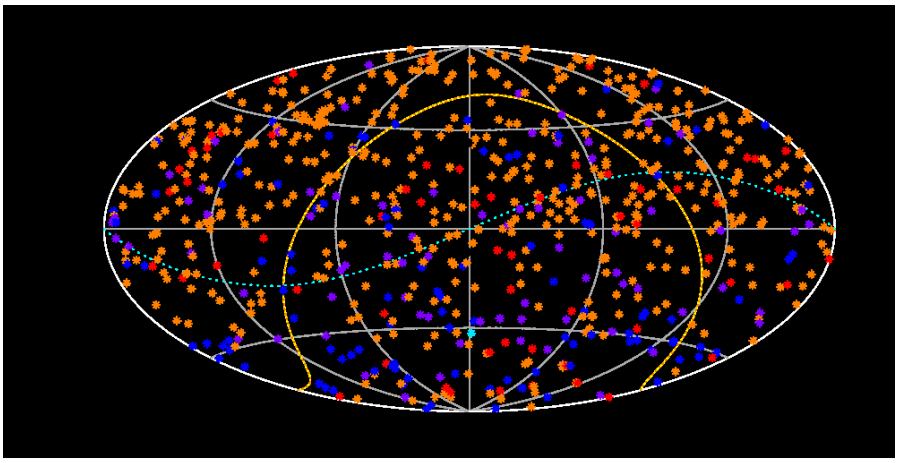

Figure 18: Distribution over the celestial sphere of the 717 ICRF sources. Individual sources are coded according to position accuracy with the following colors: orange: < 300 μas, red: 300–500 μas, purple: 500-1000 μas, blue: > 1000 μas (figure provided by C. S. Jacobs).

networks (now coordinated by the International VLBI Service for Geodesy and Astrometry). In addition, positions for another 3000 sources, determined from single-epoch measurements with the VLBA, are available from the VLBA Calibrator Survey (Kovalev et al. 2007 and references therein). A new generation VLBI frame, taking advantage of modelling improvements since the time the ICRF was built (1995), and adding the most recent data, is currently under study with plans for completion by 2009. This new frame might reach an accuracy ≤ 100 μas in the individual source positions.

The extragalactic frame derived from VLBI has been unrivalled since astrometric accuracy at other wavelengths does not reach that of the VLBI technique. At optical wavelengths, the position accuracies have been typically limited to tens of mas, as determined from ground-based observations, because extragalactic objects are faint and were out of reach of Hipparcos. The situation, however, will change in the future with the launch by 2011 of the space astrometric mission GAIA, dedicated to survey all galactic and extragalactic objects brighter than magnitude 20. At this magnitude limit, it is expected that about one billion stars and 500,000 QSOs should be detected, with position accuracies ranging from 20 μas at magnitude 18 to about 300 μas at magnitude 20. Of these, a *clean sample* of roughly 10,000 QSOs with high astrometric quality may be selected to define the GAIA frame with the highest accuracy (Mignard 2002). This frame will thus surpass the present ICRF both in accuracy and in sky density. It is anticipated that preliminary GAIA results will be available by 2015 with the final GAIA catalog published by 2020.

On the VLBI forefront, a new concept of small (12 m diameter) fast-moving antennas (20 seconds to go across the sky) and broadband delay observing (2–15 GHz continuous bandwidth) is being developed within the geodetic community, to multiply the number of observations within any given session, and thereby increase the overall accuracy of the estimated geodetic and astrometric parameters. The ultimate goal is to set up a network of 40 such antennas throughout the world, operating continuously to monitor the Earth's rotation with increased time sampling and accuracy. At the same time, this network will also have the capability to re-observe the complete ICRF (including imaging of source structures) on a daily basis, and to control the errors of the source positions and the variability of their structures. Its sensitivity, however, will still

be limited to about 100–200 mJy and a significant increase in the number of sources is therefore not planned.

In the future, the densification of the celestial frame will still rely on higher-sensitivity networks. The upgraded EVN with its large dishes (including the Yebes antenna and the SRT) and increased bandwidth should play a major role here. For example, target sources as weak as 5 mJy may be detected with SNR=15 (as required for astrometry) on baselines to Effelsberg when a recording rate of 8 Gb/s is available. Based on statistics from the NVSS, it is estimated that there are about 100,000 such sources detectable by VLBI at 8 GHz, which is comparable to the number of QSOs to be detected by GAIA. The future EVN will thus have the necessary sensitivity to build up the radio counterpart of the GAIA frame. Innovative observing techniques should be developed in this direction, e.g. within the framework of RadioNet, to make such large-scale surveys a reality.

12 The structure of the Milky Way

The structure and the dynamics of the Milky Way are still not known with high certainty. Most conclusions about Galactic structure are based on measurements of radial velocities, and transforming from velocity to distance is problematic. For example, the kinematic distance to the massive star-forming region W3(OH) is 4.3 kpc, whereas the trigonometric parallax is 2.0 kpc. To improve our knowledge about the Milky Way, it is important to measure distances and proper motions of sources with distances greater than the $\sim$ 0.1 kpc range of *Hipparcos*. Distances and proper motions of massive star-forming regions $>$ 1 kpc from the Sun would 1) locate the nearer spiral arms; 2) constrain models of the rotation of the Milky Way, which is closely related to its gravitational potential; and 3) test predictions made by spiral density wave theory, which is important for the formation and evolution of spiral galaxies in general. Future optical space missions like *Gaia* and *SIM* are planned to measure motions and distances for up to one billion stars in the next decade. However, optical astrometry missions can not probe parts of the galaxy that are obscured by dust. Thus, these missions will not be able to probe in the plane of the Milky Way beyond 1 or 2 kpc inward from the Sun. On the other hand, using VLBI techniques, one can now measure accurate parallaxes and proper motions with accuracies of 10 μas and 1 km s^{-1}, respectively. Thus, sources 10 kpc from the Sun can have distances measured with $\sim$ 10% uncertainty – a 100-fold improvement on *Hipparcos* ! Since VLBI observations of masers at cm-wavelengths are not hindered by dust, results from these observations will continue to be important even in

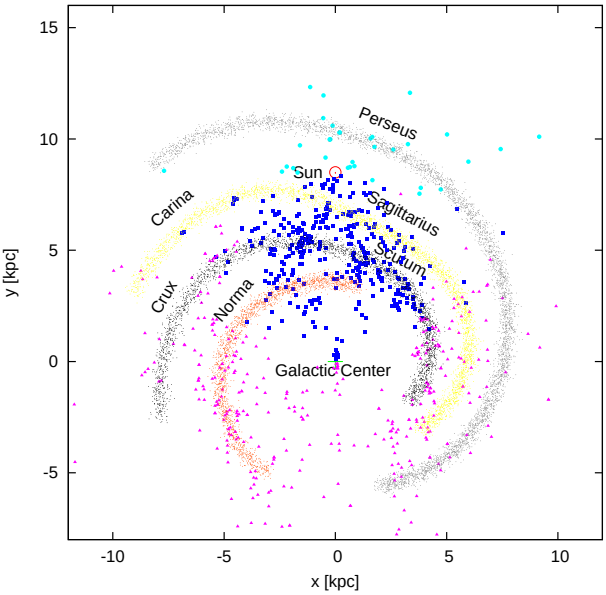

Figure 19: Positions of 6.7 GHz methanol masers at near (squares) and far (triangles) kinematic distances in the Galactic plane. The remainder (circles) is located outer the solar circle.

the GAIA/SIM era.

Galactic maser sources are compact and strong enough for VLBI, and they are located in massive star-forming regions in the Galactic disk. H_2O and methanol masers are widespread, strong, and compact. Water masers are often found in fast outflows (up to several 10 km s^{-1}), that makes an accurate determination of the total proper motion difficult. H_2O masers are also short lived (usually a few months), very variable and difficult to use for parallax observations that optimally require greater than 1 year's observations. Methanol masers are less variable, have a longer lifetime and the maser features have lower intrinsic motions. Thus, methanol masers are much better target sources to study the structure and rotation of the Milky Way. The 12 GHz transition is not very common and the number of potential target sources is limited. However, the 6.7 GHz transition is found in numerous sites in the Milky Way (Fig. 19), and the EVN is the only instrument that can observe this transition with high-resolution. This presents the EVN with a unique opportunity to make a dramatic contribution to the study of the Milky Way.

On the other hand, the large sensitivity of the EVN from the combination of large telescopes and high data rates will also allow accurate astrometry of weak continuum sources (e.g. radio stars, young stellar objects) in our Galaxy.

Phase-referencing has become a standard technique in VLBI to measure accurate relative positions of radio sources. The major error source for phase-referencing VLBI observations is the unknown propagation delay through the atmosphere for each antenna. One method to estimate the zenith delay offset is to configure the frequency bands to achieve the greatest spanned bandwidth allowed by the electronics. This allows measurement of a true *group delay* of the signals with the highest accuracy. One observes typically a dozen bright compact extragalactic radio sources (quasars), whose positions are known to better than 1 mas, in rapid succession both before and after the phase-referencing observations. The collection of multi-band delays are then fitted with a model that has parameters for the zenith delay offset and its time derivative for all antennas, as well as a clock offset and its time derivative for all antennas, except for one reference antenna. While in-beam water vapour radiometers can be also used for tropospheric calibration, it can not correct clock offsets and drifts.

A more flexible scheduling (e.g. observations at the maximum of the parallax signal) and more long baselines are needed to achieve the highest possible astrometric accuracy for the EVN2015.

References to Chapter B

Baan, W.A. 2007, NewAR, 51, 149

Baan, W.A. 2008, *Astrophysical Masers and their Environments*, IAU 242, Chapman & Baan, eds. (Cambridge University), in the press, arXiv:Astro-ph/0709.3441

Baan, W.A., Haschick, A.D., & Henkel, C. 1989, *ApJ*, 346, 680 Baan, W.A., et al. 2008, *A&A*, in preparation. Baan, W.A., Rhoads, J., Fisher, K., Altschuler, D.R. & Haschick, A., 1992, *ApJL*, 396, L99

Barvainis, R. & Antonucci, R. 2005, *ApJL* 628, L89

Beswick, R.J. et al, 2006, MNRAS, 369, 1221

Braatz, J.A. et al. 2004, *ApJL* 617, L29

Briggs, F.H. 1998, *A&A* 336, 815

Claussen, M.J., Diamond, P.J., Braatz, J.A., Wilson, A.S. & Henkel, C. 1998, *ApJL* 500, L129

Claussen, M.J., Heiligman, G.M., & Lo, K.Y 1984, *Nature* 310, 298

Darling, J. & Giovanelli, R., 2001, *AJ*, 121, 1278

Fenech, D. 2007, Ph.D. thesis, The University of Manchester

Fey, A.L., Ma, C., Arias, E.F., Charlot, P., Feissel-Vernier, M., Gontier, A.-M., Jacobs, C.S., Li, J., MacMillan, D.S., 2004, AJ, 127, 3587
Greenhill, L.J. 2007, *Astrophysical Masers and their Environments*, IAU 242, Chapman & Baan, eds. (CUP), in the press, arXiv:Astro-ph/0708.0423
Haschick, A.D., Baan, W.A. & Peng, E.W. 1994, *ApJ* 437, L35
Henkel, C., Peck, A.B., Tarchi, A., Nagar, N.M. et al. 2005, *A&A* 436, 75
Henkel, C. & Wilson, T.L. 1990, *A&A* 229, 431
Herrnstein, J.R., Moran, J.M., Greenhill, L.J., Diamond, P.J., et al. 1999, *Nature* 400, 539
Kovalev, Y.Y., Petrov, L., Fomalont, E.B., Gordon, D., 2007, AJ, 133, 1236
Lonsdale, C.J., Diamond, P.J., Thrall, H., Smith, H.E. & Lonsdale, C.J. 2006, *ApJ*, 647, 185
Martí-Vidal, I., Marcaide, J. & Alberdi, A. 2006, *LNEA*, 2, 215
Mignard, F., 2002, In: GAIA: A European Space Project, Eds. O. Bienaymé and C. Turon, EAS Publication series, Vol. 2, 327
Morganti, R. et al. 2004, *Science with the Square Kilometre Array*, C. Carilli & S. Rawlings, eds., *New Astronomy Reviews*, 48, 11
Morganti R., Tadhunter C.N., Oosterloo T. 2005, A&A 444, 9
Muxlow, T.W.B., et al. 2005, MmSAI, 76, 586
Muxlow, T.W.B., et al. 2006, MNRAS, 358, 1159
Nakai, N., Inoue, M., & Miyoshi, M. 1993, *Nature* 361, 45
Ma, C., Arias, E.F., Eubanks, T.M., Fey, A.L., Gontier, A.-M., Jacobs, C.S., Sovers, O.J., Archinal, B.A., Charlot, P.: 1998, AJ, 116, 516
Parra, R., Conway, J.E., Elitzur, M. & Pihlström, Y.M. 2005, *A&A*, 443, 383
Parra, R., Conway, J.E., Diamond, P.J., et al. 2007, *ApJ*, 659, 314
Pihlström, Y.M., Baan, W.A., Darling, J. Klöckner, H.-R. 2005, *ApJ*, 618, 705
Rovilos, E., Diamond, P.J., Lonsdale, C.J., et al. 2003, *MNRAS*, 342, 373
Rovilos, E., Diamond, P.J., Lonsdale, C.J. et al. 2005, *MNRAS*, 359, 827
Sanders, D.B. et al, 1988, ApJ, 325, 74
Seymour, N. et al. 2007, arXiv:Astro-ph/0612134, MNRAS, submitted.
Tarchi, A., Henkel, C., Peck, A.B., Menten, K.M. 2002, *A&A* 389, L39
Tarchi, A., Henkel, C., Chiaberge, M., Menten, K.M. 2003, *A&A* 407, L33

Science Case C
From Stars to Planets

13 The birth of stars and planets

Star-formation models now include sufficient factors (chemistry, magnetic permeability, geometry, turbulence etc.) to model cloud collapse and stellar condensation on the observed timescales. The mechanisms determining the IMF (e.g. metallicity, nature of the trigger) are not so predictable, and vital questions include whether massive stars are formed by the coalescence of smaller protostars, and what determines whether and how planets form. Massive YSOs severely disrupt their environment; how strongly does this affect ongoing star-formation? Resolving stellar binaries at the core stage would also be very interesting. It is not clear what determines the number and separation of stars formed during the fragmentation of a collapsing cloud, nor whether circum-binary proto-planetary discs are likely to occur.

The GLIMPSE (mid-IR), CORNISH (5-GHz HII regions) and MMB (methanol maser) surveys will give a thorough picture of star-formation in the Galactic plane at a resolution of several arcsec-arcmin. High-resolution follow-up of subsamples is vital to provide diagnostics for disentangling the mass, age and other properties of young stars in order to allow a complete census and an accurate test of how the IMF and the star-formation rate depends on location/metallicity, large-scale matter and magnetic density. This relies on radio–sub-mm observations of highly obscured regions. Unfortunately, most low-mass YSOs are sub-mJy continuum sources, detectable by the VLA but requiring ultra-deep observations by long-baseline interferometry at present. The MERLIN deep fields resolved many Orion proplyds but only one YSO in NGC 1333 despite 2–3 weeks on source.

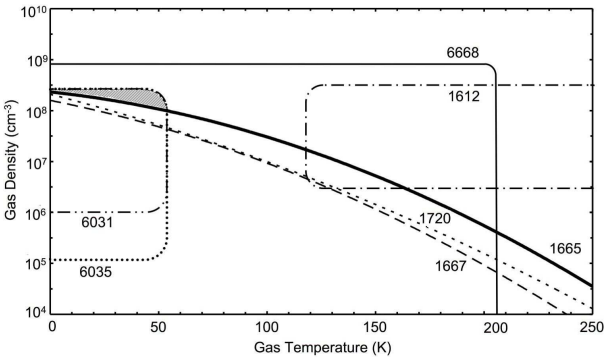

Figure 20: Physical conditions for the amplification of various OH and methanol maser lines (from Green et al. 2007, after Cragg, Sobolev and Godfrey 2005 and references therein). Multiple transitions observed from the same region provide tight constraints on the local environment.

13.1 Cloud collapse is traced by OH and methanol masers.

1. The various transitions are thought to appear and disappear in an overlapping sequence determined by the amount of each species arising from ice mantle evaporation and the pumping conditions (temperature, number density etc.; see Fig. 20). This can be used to constrain the evolutionary stage of cloud collapse as well as the physical conditions.

2. Some transitions are associated on the scale of hundreds but not tens of AU: VLBI resolution is needed to confirm co-propagation, which can constrain local physical conditions very precisely.

3. OH and methanol masers are found in many bands (some transitions are shown in Fig. 20,

labelled in MHz) which facilitates frequency flexibility.

4. Zeeman splitting of OH has confirmed the role of magnetic fields, at first controlling the collapse rate and then becoming wound into protostellar discs (e.g. Gray, Hutawarakorn & Cohen 2003). The situation at later stages is more complicated due to internal Faraday rotation. This can be alleviated by data from multiple transitions and also from 22-GHz water masers.

5. The magnetic field strengths measured from water masers are higher than those seen in nearby OH masers in both SFR and CSE. More high-resolution data are needed to confirm that this is probably due to the former tracing a denser environment.

6. Star-forming regions are concentrated in the plane of the Galaxy at low declination. This makes N-S baselines important at the location of the EVN but does allow a common sky with ALMA and other southern-hemisphere instruments.

7. Water and methanol polarization measurements require very high spectral and spatial resolution.

8. VLBI data should be complemented by shorter baselines for OH and methanol as very extended filaments up to a thousand AU have also been detected.

9. Co-propagation, Faraday rotation and other multi-transition experiments, as well as proper motion measurements, need observations as close as possible in time or regularly spaced. e-VLBI will be very helpful in being able to confirm whether a session has been a success or needs to be repeated.

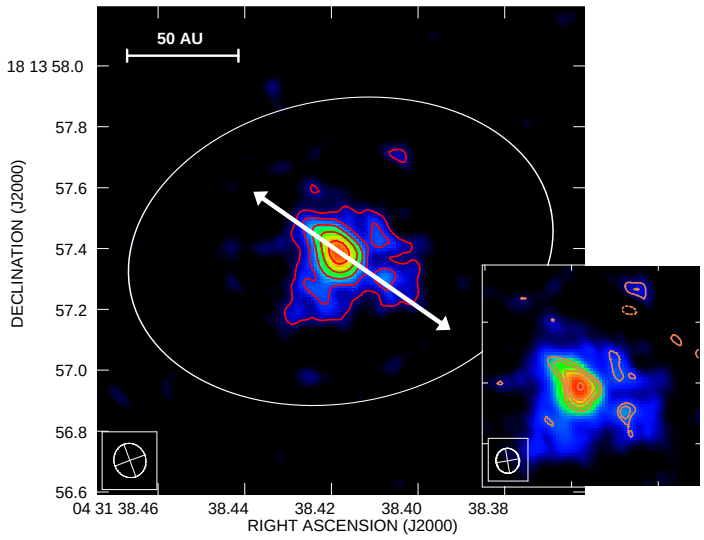

Figure 21: VLA plus Pie Town 22-GHz image of HL Tau. The mm–cm spectral index shows free-free emission from the NW jet but the disc contains large dust grains (Greaves et al. 2007).

10. Near-simultaneous continuum observations, with a maximum bandwidth much greater than the total spectral bandwidth, are needed for satisfactory observations of calibration sources. This will provide precise astrometry for co-propagation, parallax and proper motion measurements, and allow detection of the fainter masers associated with lower-mass YSO.

11. The very bright methanol and water masers are detectable in micro-arcsec beams, so very long baselines, especially N-S, would allow proper motions to be measured in months rather than years, with sufficient accuracy to disentangle local and bulk motions.

13.2 Proto-planetary discs

The study of potential planet-forming condensations is a paradigm for demanding continuum observations. Very few discs around low-mass YSO within a few hundred pc can currently be resolved into a proto-planetary disc (thermal emission from dust), and free-free emission from

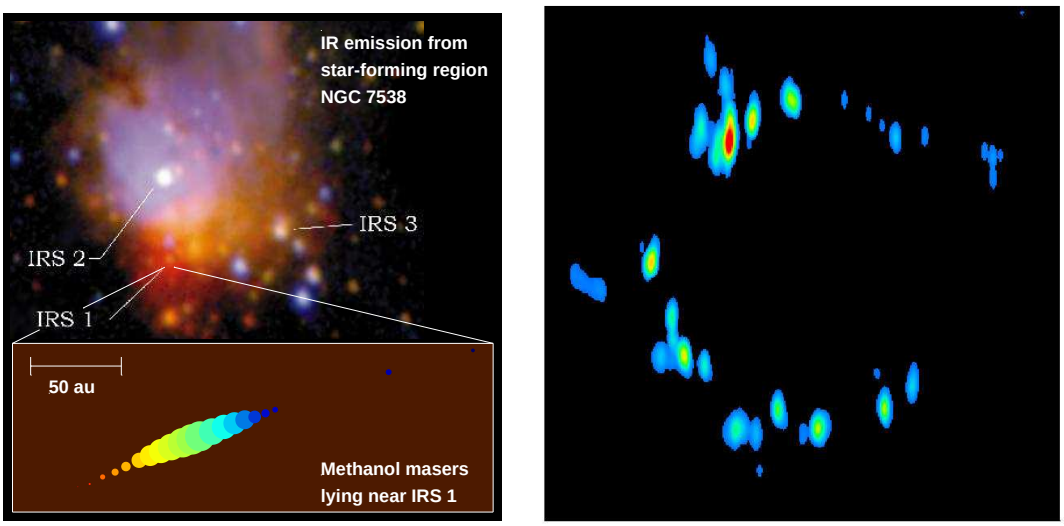

Figure 22: *Left* Methanol masers possibly lying in a YSO disc in NGC 7538 superimposed on the IR emission (Minnier, Booth & Conway, 1998; IR image courtesy of Wright, in Bloomer et al. 1998). High-resolution continuum imaging and maser proper motions are needed to distinguish between outflows, disc winds and Keplerian or expanding/infalling discs. *Right* A 150-mas radius methanol maser ring in high-mass protostar G23.657-0.127 (Bartkiewicz, Szymczak & van Langevelde 2005).

the ablation of the edges of such a disc and/or protostellar jets (Fig. 21). If multi-frequency observations at cm- and mm-wavelengths would have a resolution of a few AU, then not only could we distinguish between thermal and non-thermal components but also track the size-evolution of grains.

A condensing planetesimal in an orbit like that of Pluto would travel 1 AU in 1 year around a solar-mass star, corresponding to 2.5 mas yr^{-1} at 400 pc. The faint NE blob in Fig. 21 is such a candidate. This could be measured optimally at 12–15 GHz, but probably at a wider range of frequencies if necessary.

Easy multi-epoch proper motion measurements with the EVN2015 would facilitate establishing the controversial nature of water and methanol masers in Keplerian discs (Fig. 22). The EVN2015 e-VLBI capability and ALMA (both with short-baseline fill-in and combinations to provide matching resolution) are essential for this research.

13.3 Thermal lines

A number of thermal molecular lines have been mapped by the VLA, notably NH_3 and CCS, at frequencies above 22 GHz (Fig. 23). These lines serve as a thermometer for the very earliest stages of star-formation as well as the high-resolution kinematic information, and also test the chronology of chemical models. Unfortunately, typical flux densities are 100–200 mJy in a 4" beam in 1 km s^{-1} (absorption is usually also weak).

1. Even at the maximum thermal line width (4–5 km s^{-1}), VLBI resolution will only give a few μJy rms in a day. Nonetheless, exceptional experiments using all available antennas (including e-MERLIN, EVLA etc.) would be worth considering for exceptional objects. For example, in a

5-mas synthesised beam, using 3.5 km s−1 channels at 22 GHz, with 48 hr on-source, a 10 μJy or better (5σ) might be reached. This would be dependent on good weather.

Radio recombination lines are found at a number of frequencies down to 8 GHz or less. These trace excited regions/shocks associated with star-formation and PNe, but are typically even weaker than molecular lines. Sources are often spread over very wide regions (arcmin).

The EVN2015 should provide frequency coverage to meet ALMA at 30 GHz or above.

13.4 Planet-finding using reflex stellar proper motion

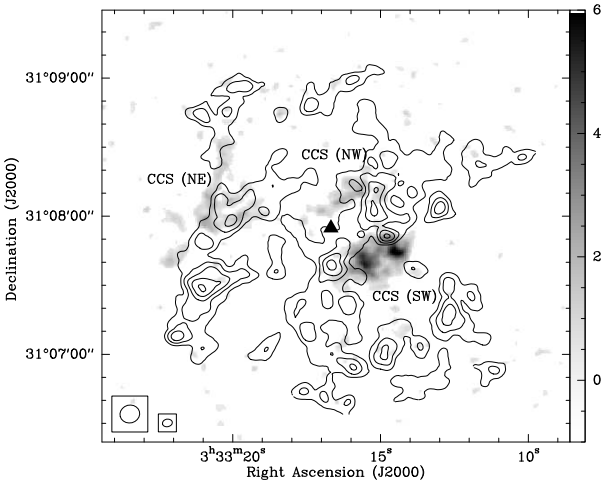

Figure 23: Ammonia (grey scale) and CCS masers around B1 IRS imaged by de Gregorio-Monsalvo et al. (2005) using the VLA.

The most obvious candidates for planet-finding are low-mass dMe stars, that are strongly perturbed by planets and magnetically active. They are radio-bright (for stars) but exhibit a high level of intrinsic optical line velocity dispersion, which makes them unsuitable for traditional radial velocity searches (Guirado et al. 2002). The radio emission region is not necessarily point-like at VLBI resolution, but the effects of wind activity and planet-related motion can, in principle, be disentangled (Pestalozzi 2000; Pestalozzi et al. 2000).

At least one similar M-dwarf has a planetary companion, OGLE 2005-BLG-390Lb, identified by microlensing (Cassan & Kubas 2006). There are 34 M-dwarfs within 5 pc, with typical proper motions of a few hundred mas per year. Nine of these have stellar-mass companions (Leinert et al. 1997), but the rest would be more straightforward candidates for planet-finding. There are about 500 active M-dwarfs within 50 pc (Riaz, Gizis & Harvin, 2006) and micro-arcsec perturbations would be detectable, especially if any are in the vicinity of good ICRF calibrators.

The EVN2015 provides the required technical accuracy as described for other astrometry projects. The main unforseen issues are likely to arise in developing suitable models. The EVN2015 and eEVN will allow the regular measuring of positions and, possibly more important, the rapid response to triggers that indicate that an active star is in a suitable and observable state.

14 Celestial recycling

The bulk of the material returned to the ISM, enriched in elements heavier than He, arises from middle-aged stars after leaving the main sequence, but before the final collapse into a compact object involving SNe or PNe. The conditions controlling the next generation of star-formation (cooling, magnetisability, IMF etc.) are determined by the chemical composition, both elemental and molecular, of gas and dust ejected by stars, and mediated by ISM processing. Hot topics include the questions of (a) under what conditions can planets of various types form, and (b)

what provided the first dust in the universe: SNe or red supergiants or Wolf-Rayet stars (WR)? The higher the mass of a star, the more sensitively its lifetime depends on the mass loss rate in various stages, further influenced by binarity. This process is not well-understood, but determines the rate of long-term conversion of galactic material into stars. Almost all PNe and indeed circumstellar envelopes have some degree of asymmetry, but some have solitary progenitors with no detectable surface rotation in the AGB/RSG phase. Magnetic forces can be measured but that just shifts the mystery to the origin of an ordered field.

Masers studies provide astonishingly high-resolution and 1 AU at 10 kpc is already achievable. A combination of parallax and proper motion measurements provide highly accurate distances, such as those obtained for U Her (Vlemmings et al. 2003) and the recent VERA results. SiO masers have recently been detected in single-dish observations of globular clusters, and VLBI at 43 GHz may become a standard means of fixing their distance and kinematics.

Thermal and non-thermal radio continuum emission traces the interactions between winds in low-mass symbiotic binaries and Wolf-Rayet stars. The high-energy phenomena of SNe and XRB are covered separately as Cosmic Power Sources.

14.1 Molecules and dust from cool stars

From the stellar surface outwards, AGB stars and RSG are very similar. They differ mainly by an order of magnitude in scale, with a stellar radius $R_\star$ typically 1 and 10 AU respectively, and they have water maser clouds of similar sizes in shells extending from a few to a few tens $R_\star$. RSG have mass loss rates typically 10 times higher than AGB stars, which suggests that the mass loss process is determined by macroscopic stellar processes. This is in contrast to microphysics that determines the maser line width – common to all objects for a given saturation state – or the wind expansion velocity, varying by a factor of only a few as determined largely by the dust composition and optical depth. Is mass loss concentrated in a few $\sim M_\oplus$ parcels per stellar period (one–few years)? The surface of α Ori has structure on large scales which could correspond to clumps of star spots or other magnetic phenomena, and/or convection cells (Freytag 2003 and references therein), possibly chemically enriched by dredge-up. Tracking matter from the stellar surface into the wind using a range of molecular species and instruments will provide answers to these questions.

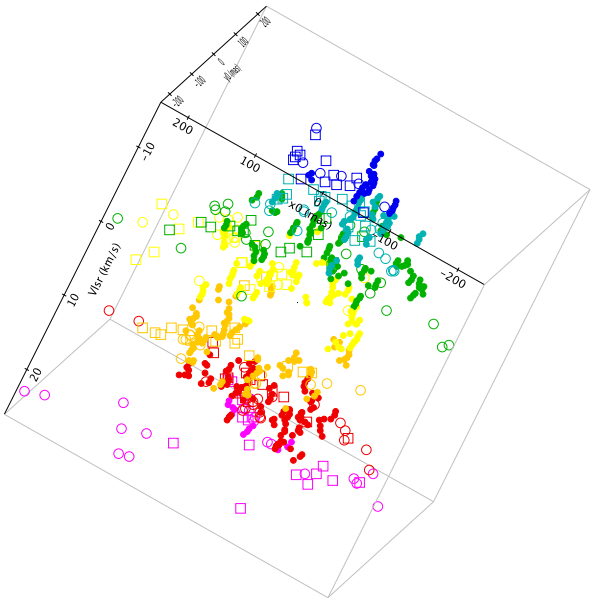

Figure 24: EVN/Global VLBI positions on OH mainline masers (open symbols) and MERLIN water masers (solid symbols) around VX Sgr. The shade represents velocity with respect to the star, showing that the masers are interleaved but not exactly co-spatial (Murakawa et al. 2003; Richards 2006; additional data from Masheder and Bartkiewicz).

1. The photosphere and chromosphere of some of the closest AGB stars (e.g. W Hya, RT

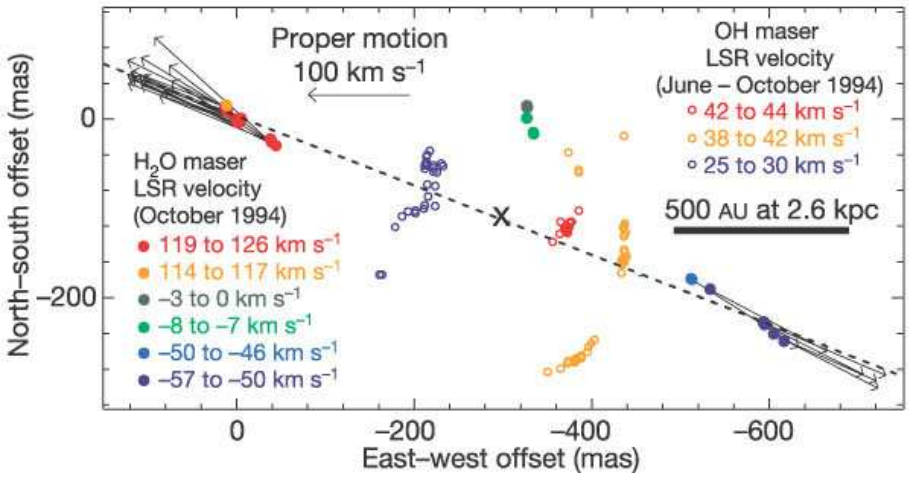

Figure 25: The magnetically collimated 'water fountain' W43A (Vlemmings, Diamond & Imai, 2006; Imai et al. 2002).

Vir, U Her) and RSG (e.g. VX Sgr) will be resolved by deep observations using a full range of baseline lengths. The surface brightness is 2000 – 3000 K, probably with non-thermal radio-bright regions, but variability will limit individual observations to a day or so. Phase-referencing using SiO or water masers (43 and 22 GHz) should be possible, but lower frequencies down to 5 GHz would disentangle thermal and non-thermal regions.

2. SiO masers form within $\sim 2\ R_\star$ so, at an expansion velocity of 5 km s$-$1, a clump might appear at 2 AU from the stellar surface 2 years after its ejection. Alternatively, the appearance of masering components might be determined within 10–20 mins by local changes in stellar radiation.

3. Dust forms at 4–8 $R_\star$ but a complicated feed-back system related to the stellar period, including superperiods, has been suggested.

4. Water masers also appear at a similar distance from the star and a major question is whether they, and the dust, condense in co-spatial clumps, and if so, what binds these clumps? Is it local chemistry (cooling catastrophe?), magnetic forces or some other agent?

5. OH mainline masers appear in between the water masers in some sources, contrary to the simplest models based on low-resolution data (Fig. 24). Contemporaneous monitoring will show whether they are closely associated (e.g. dissipating edges of water maser clouds) or more widely separated. Do they form from discrete clumps, or from more tenuous, extended gas? Are they associated with a lower-density polar outflow?

6. OH 1612-MHz masers form a shell outside the water masers. However, a few objects have shown 1612-MHz eruptions at close to the stellar velocity (e.g. Etoka & Le Squeren 1996), suggesting a separate origin in the inner CSE related to stellar flares.

7. Axi-symmetry is most pronounced in post-AGB objects. PPNe typically show either bipolar water fountains (e.g. Fig. 25, Vlemmings, Diamond & Imai 2006) with equatorial OH masers, or biconical and equatorial OH masers with stronger emission at 1667 MHz, overshooting the 1612 MHz velocity extent (e.g. Zijlstra et al. 2001; Bains et al. 2003). Some axi-symmetry is seen in the AGB/RSG stage, for example the lower-density bi-cone in VX Sgr (Fig. 24), which coincides with the magnetic axis (Murakawa et al. 2003).

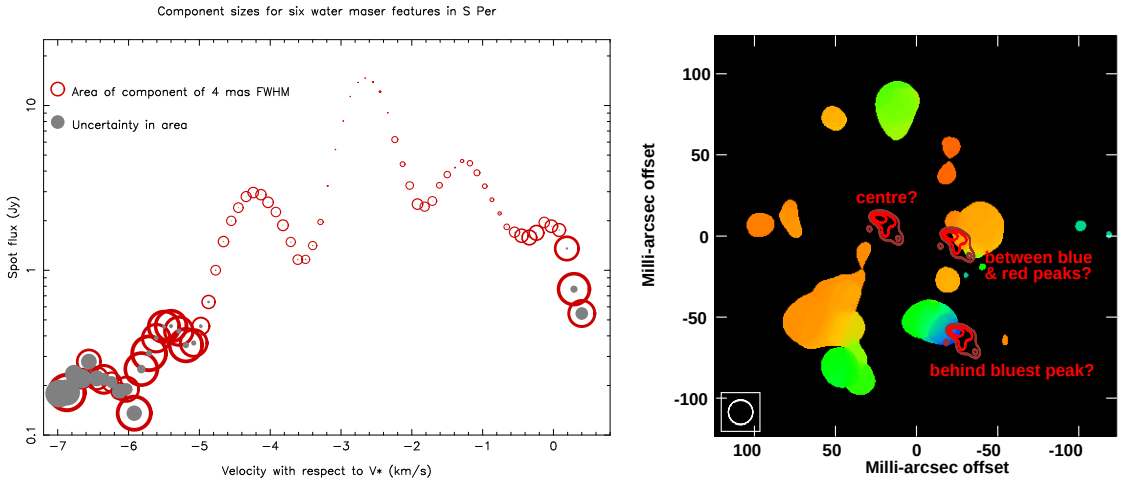

Figure 26: *Left* The variation of maser component size in spectral channels across a single maser cloud about 40 AU in size (Richards, Yates & Cohen 1999). *Right* Possible locations of U Her in its water maser shell imaged by MERLIN (from Richards et al.)

14.2 Maser physics

VLBI and MERLIN combined can measure the sizes of maser spots in separate channels (the beamed size) and the total size of the masering clump across several velocity channels (Fig. 26 *Left*). Size information tests the fundamental assumptions of maser physics and the diagnostics of the saturation state such as:

1. the relationship between the beaming angle and the geometry and velocity structure of the emission region, 2. the narrowing of the beaming angle with intensity and saturation, 3. narrowing and rebroadening of the line width, 4. shrinking of the maser spot size towards a line peak, compared with the wings, 5. distinguishing between masers emanating from quasi-spherical clouds (which are expected to appear narrower with increasing brightness) and from shocked slabs (which may retain their original size), and, 6. the interpretation of maser polarization is highly controversial yet vital for reconstructing the underlying magnetic field strength and orientation.

The EVN2015 provides a more sensitive VLBI system without correlator limitations and allows better measurements of the small (few percent) polarization of water masers. The EVN2015 with e-MERLIN will improve high-resolution measurements of OH maser polarization without spatial blending or beam depolarization. It will become possible to compare measurements of different lines close in time, which will reveal any internal Faraday rotation (such as due to higher fractional ionization close to the star or in a bi-conical outflow).

14.3 Tracing mass loss from the stellar surface

An ideal program to study the activity at the stellar surface would be to observe the star (VLTI, ALMA, VLBI plus e-MERLIN, EVLA) and SiO masers (VLBI) every week for a few weeks, and then continue observing both or just the SiO until (and if) changes could be related. Extensive long-term data has already been taken by Diamond et al. on the variability, proper motions and polarization on SiO masers. However, the SiO-dust-water transition would be investigated using VLBI, ALMA and VLBI plus e-MERLIN, respectively, ideally every few weeks for a year or two,

to monitor changes with position in the wind and with stellar period.

Water maser monitoring suggests that the main force on the wind is an outward expansion but there are hints of preferred directions and axi-symmetry. Variability means that single epochs are misleading. It is also mostly supposition that the star is at the centre of expansion (apart from W Hya; Reid & Menten 1990). Such observations will settle the location of the star with respect to SiO and water masers (Fig. 26 *Right*). VLBI alone is good for proper motions and also magnetic field measurements. OH masers are more seriously resolved and e-MERLIN fill-in will be needed to prevent imaging artifacts as well as to reveal more diffuse masers. VLBI is vital to measure OH proper motions and thus test models of bi-conical outflow (Zijlstra et al. 2001) and whether the different lines co-propagate, or trace regions with different physical conditions.

Good astrometry of the EVN2015 with respect to the ICRF (International Cosmic Reference Frame) is vital to allow model-independent alignment of different species and epochs.

14.3.1 Low-mass binary star evolution and born-again systems

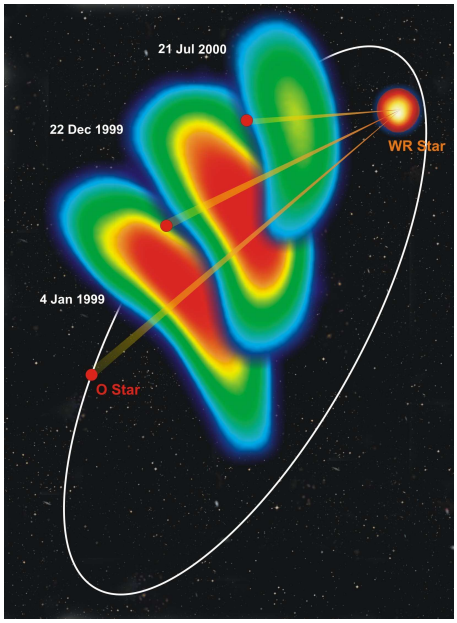

Figure 27: VLBA monitoring of the orbital motion of WR 140 at 8 GHz (Dougherty et al. 2005).

Mass transfer between binaries affects the form in which matter is returned to the ISM and in some cases the rate and nature of evolution itself. The most dramatic examples are symbiotic or recurrent novae, where accretion onto a WD from a more slowly-evolving partner may change the nuclear composition (producing prodigious C-rich dust) and eventually may become a Type-Ia supernova. Other objects undergo evolutionary loops (e.g. born-again novae and PNe like VY Mon and Sakurai's object), which current theories cannot predict and struggle to explain even after the event. It is not known how common such behaviour is, a fact which has worrying consequences for stellar population synthesis.

The main criteria for successful VLBI observations are rapid response, high-sensitivity in days or hours (in case of variability) and frequency flexibility. Coordination with e-MERLIN and EVLA will be necessary.

14.3.2 Wolf-Rayet dust factories and their progenitors

WR are responsible for much present-day Galactic carbon creation. Typical mass-loss rates from WC stars exceed 10^{-5} $M_{\odot}$ yr^{-1} of carbon, of which 1–2% is in the form of dust (Harries et al. 2004). Dougherty & Pittard (2007) review the use of VLBI to test WR models. High-resolution multi-frequency radio observations disentangle the thermal hot star wind from shocked interactions (e.g.VLA plus PT at 43 GHz compared with EVN and/or MERLIN 5-GHz observations of WR 146 and 147). Closer systems such as WR 140 (Fig. 27, orbital period 7.9 yr, separation 2-30 AU, distance about 1.8 kpc) are easier to model, as variability, spectral index and radial velocity variations can be tracked. These parameters were determined using coordinated VLBI, optical/IR interferometry (e.g. IOTA) and high-energy observations.

IR interferometry (Tuthill, Monnier & Danchi 1999) shows that the close-separation WR 104 has a nebula rotation of 0.303 mas yr^{-1}. The rotation of these more distant objects could be directly measured by the EVN, with a 4 mas beam at 6 GHz. ALMA will reveal the location as well as the orbital phase of dust formation, and its relation with the thermal and non-thermal radio-detected winds.

At least a quarter of all radio-detected O stars are binaries with non-thermal spectra and are likely to be WR progenitors. VLBI imaging can confirm this by revealing the distinctive bow shock shape of colliding wind emission. The few hundred known Galactic WR are strongly concentrated in the Galactic plane. The VLA 8-GHz WR survey (Cappa, Goss & van der Hucht 2004) detected about half of 34 candidates, with unresolved flux densities between 0.12 – 5 mJy, out to 5 kpc.

The EVN2015 will enhance greatly the area of stellar research in the following areas by:

1. Bringing the PNe and the radio continuum from post-AGB/PPNe objects within reach of high-resolution radio interferometry (in addition to the few which have masers such as W43A, Fig. 25). This will help explain major controversies like the origins of asymmetry from single progenitors, lifetimes and variability (including outbursts).

2. Delivering flux densities probably as faint as a few tens of μJy in beam sizes of order 20 mas, although e-MERLIN and EVLA fill-in and wide fields (e.g. 20 arcsec) will also be needed.

3. Testing directly the colliding winds model for PNe (Kwok, Purton & Fitzgerald 1978 and its recent revisions), by measuring detailed proper motions to see if expansion is faster along the axis of elongation, for example.

4. Providing multi-frequency spectral index measurements revealing temperature and density differences between wind components and possible shocked regions.

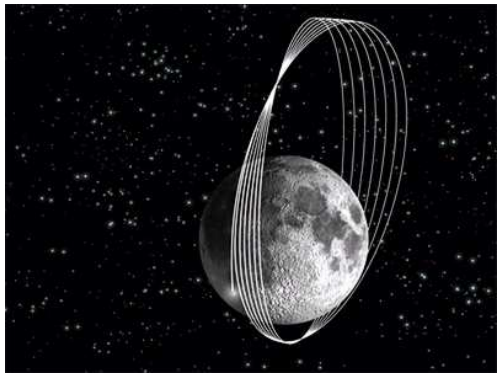

Figure 28: The trajectory of SMART1, monitored using VLBI (ESA/JIVE press release).

15 Solar system science

Spacecraft tracking has been shown to work well to 0.1-mas accuracy using normal phase-referencing to a quasar (Fig. 28). e-VLBI will come into its own here due to time-critical nature of these observations, and the fact that results are often wanted very rapidly (within 12 hours or less) after encounters with solar-system bodies or adjustments to the mission path. Existing arrays (VLBA, MERLIN, EISCAT) are used to probe the solar wind and its distortion of radio emission from background QSO, usually at 5 GHz for the cm-wave arrays. The EVN2015 e-VLBI capability will provide exact coordination and/or rapid responses. Other space-science and radar aspects are under development.

References to Chapter C

Bains, I., Gledhill, T.M., Yates, J.A., Richards, A.M.S., 2003, MNRAS, 338, 287
Bartkiewicz, A, Szymczak, M., van Langevelde, H.J., 2005, A&A, 42, 61
Bloomer, J.D. et al., 1998, ApJ, 506, 727

Cappa, C., Goss, W.M., van der Hucht, K.A., 2004, AJ, 127, 2885
Cassan, A., Kubas, D., 2006, "Transiting Extrasolar Planets Workshop", Ed. C. Afonso & D. Weldrake, ASP Conf. Ser, astro-ph/0621014
Cragg, D.M., Sobolev, A.M., Godfrey, P.D., 2005, MNRAS, 360 533
de Gregorio-Monsalvo, I., Chandler, C.J., Gómez, J.F., Kuiper, T.B.H., Torrelles, J.M., Anglada, G. 2005, ApJ, 628, 789
Dougherty, S.M., Pittard, J.M., 2006, "8th EVN Symposium", Ed. A. Marecki et al., PoS http://pos.sissa.it//archive/conferences/036/049/8thEVN_049.pdf)
Dougherty, S.M., Beasley, A.J., Claussen, M.J., Zauderer, B.A., Bolingbroke, N.J., 2005, ApJ, 623, 447
Etoka, S., Le Squeren, A. M., 1996, A&A, 315, 134
Freytag, B., 2003, "12th Cambridge Workshop on Cool Stars", Ed. A. Brown, G.M. Harper, & T.R. Ayres, University of Colorado, 1024
Gray, M.D., Hutawarakorn, B., Cohen, R.J., 2003, MNRAS, 343, 1067
Greaves, J.S., Richards, A.M.S., Rice, W.K.M., Muxlow, T.W.B., 2007, Science, submitted.
Green, J.A., Richards, A.M.S., Vlemmings, W.H.T., Diamond, P., Cohen, R.J., 2007, MNRAS, accepted, eprint arXiv:0709.0604
Guirado, J.C., Ros, E., Jones, D.L., Alef, W., Marcaide, J.M., Preston, R.A., 2002, "6th EVN Symposium", Eds. Ros, Porcas, Lobanov, & Zensus, MPIfR, 255
Harries, T.J., Monnier, J.D., Symington, N.H., Kurosawa, R., 2004, MNRAS, 350, 565
Imai H., Obara, K., Diamond, P.J., Omodaka, T., Sasao, T. 2002, Nat. 417, 829
Kwok, S., Purton, C.R., Fitzgerald, P.M., 1978, ApJ, 219, L125
Leinert C., Henry, T., Glindemann, A., McCarthy Jr., D.W., 1997, A&A, 325, 159
Minier, V., Booth, R.S., Conway, J.E., 1998, A&A, 336, L5
Murakawa, K., Yates, J.A., Richards, A.M.S., Cohen, R.J., 2003, MNRAS, 344, 1
Pestalozzi, M.R., Benz, A.O., Conway, J.E., Güdel, M., 2000, A&A, 353, 569
Pestalozzi, M., Benz, A.O., Conway, J.E., Gudel, M., Smith, K., 2000, "5th EVN Symposium", Ed. J.E. Conway, A.G. Polatidis, R.S. Booth & Y.M. Pihlström, OSO, 167
Reid, M.J., Menten, K.M., 1990, ApJ, 360, L61
Riaz, B., Gizis, J.E., Harvin, J., 2006, AJ, 132, 866
Richards, A.M.S., 2006, "8th EVN Symposium", Ed. A. Marecki et al., PoS, http://pos.sissa.it/archive/conferences/036/042/8thEVN_042.pdf.
Richards, A.M.S., Yates, J.A., Cohen, R.J., 1999, MNRAS, 306, 954
Tuthill, P.G., Monnier, J.D., Danchi, W.C., 1999, Nat., 398, 487
Vlemmings, W.H.T., Diamond, P.J., Imai, H., 2006, Nat., 440, 58
Vlemmings, W.H.T., van Langevelde, H. J., Diamond, P. J., Habing, H.J., Schilizzi, R. T., 2003, A&A, 407, 213
Zijlstra, A.A., Chapman, J.M., te Lintel Hekkert, P., Likkel, L., Comeron, F., Norris, R.P., Molster, F.J., Cohen, R.J., 2001, MNRAS, 322, 280

Science Case D
Cosmic Power Sources

16 Accretion and outflows from relativistic objects

Accretion is a ubiquitous phenomenon associated with the force of gravity acting on all scales in the Universe, from the formation of asteroids and planets to the feeding of black holes with masses of millions or billions times the mass of our Sun in the central regions of Active Galactic Nuclei. In its most dramatic form, gravitational accretion onto relativistic objects — black holes and neutron stars — is associated with outflows of highly energetic material, which can sometimes reach speeds approaching the speed of light. The energetic particles in these high-velocity jets emit radio synchrotron radiation in the ambient magnetic fields, making high-resolution radio observations key to improving our understanding of these exotic objects and the processes occurring in them. The resolution provided by the Very Long Baseline Interferometry is unmatched in any other waveband.

16.1 Probing the compact regions of active galactic nuclei

Nuclear activity is nearly ubiquitous in galaxies, with recent observations at infrared and sub-millimetre wavelengths suggesting that virtually all massive galaxies go through a phase as an Active Galactic Nucleus (AGN) in the course of their cosmological evolution. VLBI studies have traditionally targeted primarily non-thermal synchrotron emission from the most powerful radio-loud AGNs, but continued improvements in the sensitivity attained by radio-interferometric observations have broadened the scope of investigations to a wide range of galaxies showing various levels of activity, including the nuclear region of our own Milky Way.

In the generally accepted AGN paradigm (Fig. 29), an accretion disk surrounding the central black hole, the accretion-disk corona, regions of optical-line-emitting gas (the so-called broad-line and narrow-line regions), a molecular torus surrounding the galactic nucleus and both sub-relativistic and relativistic outflows all play important roles in processes associated with the central supermassive black hole. Some infalling material is accreted onto the central object, while some is diverted to form bi-directional outflows along its rotational axis. There is a strong, compact, hot source of continuum radiation that ionizes the gas in the broad-line region, whose exact location is not known (e.g., in the accretion disk or in the hot disk corona). In addition, there is no doubt that some part of the optically-emitting gas may interact with the jet plasma, making joint high-resolution optical–radio studies of AGNs of considerable interest.

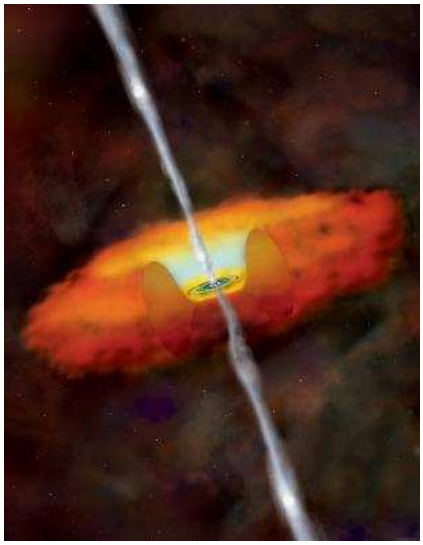

Figure 29: Schematic of the standard AGN model where a central supermassive black hole and its accretion disk eject two jets along the black-hole rotation axis. A molecular torus surrounds the central region and may block some regions of line emission for some viewing angles.

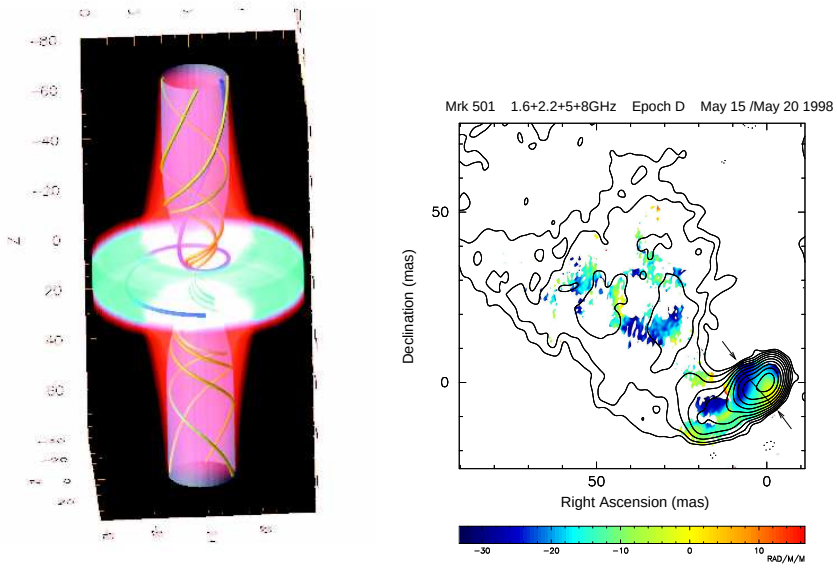

Figure 30: Left: Diagram from Casse & Keppens (2004) illustrating the generation of a helical jet magnetic field due to the combination of rotation of the central engine and the jet outflow. Right: The AGN 1652+398 (Mrk501) is one of about a dozen in which a Faraday-rotation gradient has been detected across the VLBI jet, providing direct evidence that the jet has a helical magnetic field (Croke, Gabuzda & Katz 2008). The Faraday rotation depends on the line-of-sight magnetic field, and the gradient arises due to the systematic change in the line-of-sight component of the helical magnetic field across the jet.

There is also growing evidence for the presence of a conical broad-line component, associated with a slower, sub-relativistic outflow originating in outer regions of the accretion disk. This sub-relativistic outflow is believed to be responsible for the broad absorption lines observed in a number of quasars. The disk, the broad-line region, and the jet outflows must be closely connected. Reconstructing the physical mechanisms behind this connection and understanding the physical processes in the extreme vicinity of the central supermassive black hole are pivotal to our understanding of the AGN phenomena. The only technique that can provide direct imaging on the relevant scales is VLBI.

In the coming decade, astrophysical research on AGNs will focus on a number of fundamental questions. High-resolution and high-sensitivity VLBI observations with the EVN will be one of the prime tools for this research. Specific areas of AGN research connected to the physical processes occurring on parsec and sub-parsec scales that will be addressed by EVN observations include the following.

16.1.1 The physics of relativistic jets

There is little doubt that the jets in radio-loud AGNs are highly relativistic bulk outflows; however, a number of fundamental questions currently remain unanswered. How are the jets produced and launched? What are the intrinsic flow speeds and how do they evolve with distance from the core? How are the jets collimated? The one-sided appearance of most such AGNs on the scales probed by VLBI observations is believed to be due to the relativistic beaming of each of the oppositely directed jets in the forward direction of its motion, which dramatically increases/decreases

the brightness of the approaching/receding jet. Direct information about the magnetic field giving rise to the synchrotron radiation is provided by measurements of the linear polarization of the radio emission. Although the circular polarization generated by the synchrotron mechanism is quite low (substantially less than 0.1%), measurable circular polarization (from a few tenths of a percent to a few percent) can be produced via so-called Faraday conversion of linear to circular polarization when the polarized wave passes through a magnetized plasma. Measurements of this circular polarization are technically difficult, but can provide additional information about the magnetic-field structure and composition of the conversion region.

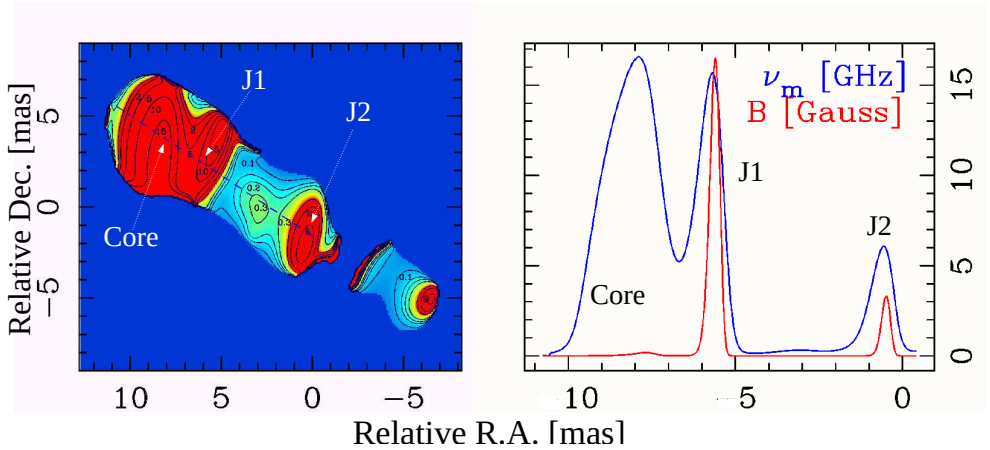

Figure 31: Left: Distribution of the synchrotron turnover frequency, $\nu_{\rm m}$, in the jet in 3C 273 obtained from multi-frequency VLBI observations. Three regions of increased $\nu_{\rm m}$ can be seen: one in the "core" and two coincident with two bright super-luminal features in the jet (denoted J1 and J2). Right: Profiles of the turnover frequency (blue) and magnetic field strength (red) taken in the jet, along the dashed line shown in the left panel. The low magnetic field in the core region indicates that the field is tangled or intrinsically weak there. The magnetic field profile shows strong spikes at the locations of the features J1 and J2, suggesting that these are most likely due to magnetic field compression in strong shocks propagating in the jet. Adapted from Lobanov (1998).

There is growing evidence that the jets of many AGNs have helical magnetic fields, suggesting, for example, magnetic collimation (Fig. 30; for a recent review, see Gabuzda 2007). Gradients in Faraday rotation have now been observed across the jets of a number of AGNs, interpreted as being due to the systematically changing line-of-sight component of the helical field across the jet. After several unsuccessful searches for correlations between the measured degrees of circular polarization in the compact VLBI core and various other observational properties in the radio, optical and X-ray, a recent analysis likewise indicates a link between this circular polarization and the presence of helical jet magnetic fields (Gabuzda et al. 2008). The increasingly likely possibility that magnetic fields and electrical currents very substantially influence the formation and evolution of the jets is very exciting. This opens completely new areas of observational and theoretical research in which high-resolution, high-sensitivity EVN observations can play a key role.

It is likely that relativistic shocks and plasma instabilities play important roles in the dynamics and evolution of the jets on somewhat larger scales. Stratification and rotation of the flow are expected to be common, but conclusive observational evidence has been elusive. High-resolution EVN observations of the internal structure of jets can address these questions, and also enable

in-depth studies of plasma instabilities. Imaging of the distribution of the turnover frequency of the spectrum can provide an excellent tool for plasma diagnostics and for distinguishing between shocks and instabilities in the jets (Lobanov 1998; Fig. 31).

Complemented with kinematic information from proper motion studies and information about the magnetic-field structure from polarization observations, this can yield detailed descriptions of these relativistic flows.

Knowledge of the radio spectra in different parts of the radio structure from multi-frequency EVN observations will also enable the identification of regions of particle acceleration or low-frequency absorption. The Faraday-rotation and circular-polarization observations provide supplementary information about the magnetic-field structure and the distribution and composition of the relativistic and thermal plasma in and surrounding the jets.

16.1.2 The jets and the nuclear regions of AGNs

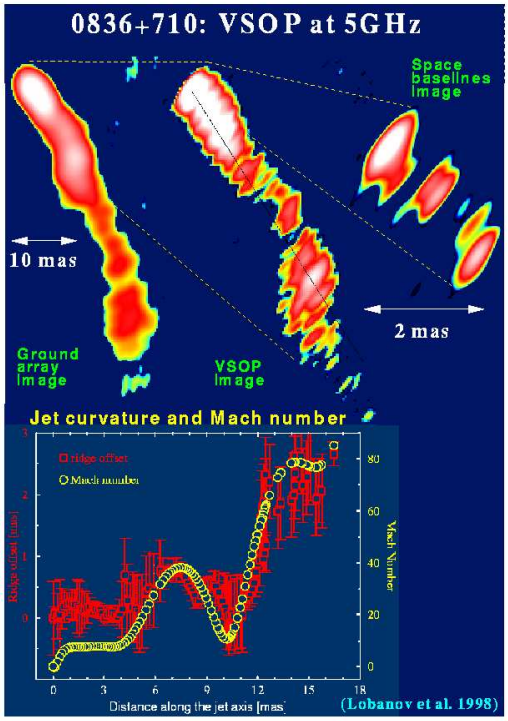

Figure 32: Images resulting from 5-GHz VSOP space VLBI observations of the quasar 0836+710 (Lobanov et al. 1998). The extra resolution provided by the space–ground baselines made it possible to study the transverse structure of the wiggling jet in considerably greater detail than had been possible previously.

The emission properties, dynamics, and evolution of the relativistic jets in AGNs are intimately related to the characteristics of the central supermassive black hole, accretion disk, and associated regions of thermal gas. Coordinated EVN, optical and X-ray observations can directly investigate these relationships; the resolution provided by the EVN is crucial in order to isolate the most compact regions of radio emission and provide information about it on the relevant scales. Such joint observations also provide the promise of estimating the masses and spins of the central black holes in AGNs, identifying the location of the non-thermal continuum source and tracing possible connections between instabilities developing in the accretion disk and the production of jets.

The EVN will be able to provide critical input by providing imaging with resolutions unsurpassed in other wavelength ranges, as well as measurements of the nuclear magnetic fields in the radio-emitting regions of AGNs on scales of $\leq 10^5$ times the gravitational radius $R_{\rm g}$.

Analysis of opacity effects, such as measurements of shifts in the position of the VLBI core — the base of the approaching relativistic jet — with frequency, is another direct source of information about the properties of the base of the relativistic flow and its environment. The properties of the circumnuclear material can be studied via analysis of the frequency dependence of the nuclear opacity, which can result from pressure and density gradients or absorption in the surrounding medium associated with the broad-line region. Changes of the nuclear opacity with

frequency can be used to estimate the size, particle density and temperature of the absorbing material surrounding the jets.

16.1.3 Atomic and molecular material in AGN

Opacity and absorption in the nuclear regions of AGN can be studied effectively with the EVN using the non-thermal continuum emission as a background source. Absorption due to several atomic and molecular species (most notably HI, CO, OH, and molecules like HCO^+) can probe the conditions in the warm neutral gas, and CO and HI absorption can be used to study the molecular tori at a linear resolution smaller than a parsec. These observations will provide detailed information about the neutral gas in AGN.

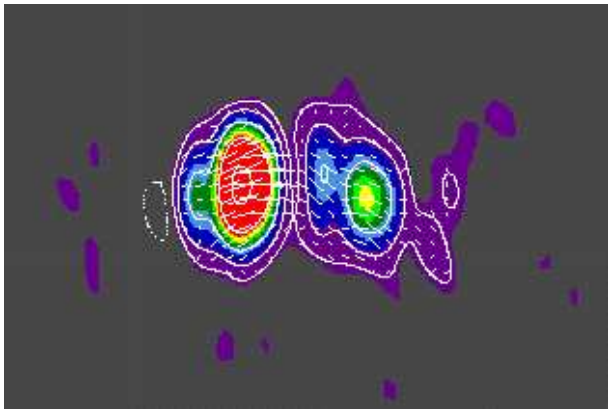

Figure 33: Image resulting from polarization-sensitive 5-GHz VSOP space VLBI observations of the AGN 1803+784 (Gabuzda 1999, 2000). The extra resolution provided by the space–ground baselines revealed appreciable bending in the innermost jet, with the polarization being well aligned with the local jet direction throughout the jet as it bends. This implies that the magnetic field is everywhere orthogonal to the jet, leading to the idea that this was the toroidal component of a helical magnetic field associated with the jet.

16.2 AGN research with EVN

In the coming decade, astrophysical research on AGN will focus on a number of fundamental questions. High-resolution and high-sensitivity VLBI observations will be one of the prime tools for research on physical processes occurring on parsec and sub-parsec scales in AGN. The success of EVN observations in addressing these and other fundamental questions of AGN physics will rely on several specific technical capabilities and new developments that are expected to be realized at the EVN within the next decade.

Monitoring programs of ultra-compact jets and the nuclear regions of AGN will require frequent EVN sessions (6–10 times a year) in order to trace rapid evolution on sub-parsec scales and provide adequate time coverage for comparisons with X-ray and optical monitoring programs.

Advanced imaging applications, such as detailed linear and circular polarization mapping, Faraday-rotation mapping, and turnover-frequency mapping, will rely on accurate calibration and improved pixel fidelity of images obtained from EVN data, as well as improved frequency coverage and frequency agility.

Studies of the internal structure of jets will require regular availability of transcontinental baselines and accurate calibration.

Two important challenges for continuing the scientific success of EVN will be ensuring sufficient fidelity of EVN data and developing novel and creative techniques for extracting information from VLBI images. Future advances in all aspects of high-resolution studies will require pixel-based interpretation of data (as opposed to the "blob-based" interpretation most commonly used at present). Currently, most information inferred from VLBI data is essentially one-dimensional (flux variations, spectra, trajectories, strip profiles of the brightness, spectral index or degree

of polarization), which severely limits the cross-over between data and theory. Searches for solutions to this problem should be focused on finding ways to extract reliable two-dimensional information from images. This approach will depend strongly on high-fidelity imaging and novel reduction and analysis techniques for the continuous extraction of information from interferometric images: mapping the velocity fields and spectral and magnetic-field distributions; and developing advanced two-dimensional correlation functions, as well as pattern-recognition and pattern-tracing algorithms.

16.3 AGNs at the highest resolution – mm VLBI and space VLBI

The driving motivation to perform VLBI at the highest possible frequencies comes from the corresponding increase in angular resolution, which is proportional to λ/B (wavelength λ and antenna separation B; for a recent review, see Krichbaum 2007). For ground-based VLBI, the diameter of the Earth sets an upper limit to the antenna separation, which necessitates observations at the shortest possible wavelengths, if one aims to image the most compact and energetic regions in extragalactic radio sources. Although space-VLBI observations with one or more orbiting radio antennas could overcome the limitation posed by the Earth's diameter, cost considerations are likely to limit the diameters of any such space antennas to $D \lesssim 20\,\mathrm{m}$, leading to sensitivity limitations for space-VLBI observations in the foreseeable future. Therefore, ground-based VLBI operating at short mm-wavelengths ($\lambda \leq 7\,\mathrm{mm}$) and space-VLBI operating at longer wavelengths ($\lambda \geq 7\,\mathrm{mm}$) complement each other through their different observing bands, resolutions, sensitivities and special capabilities with regard to specific scientific questions (Figs. 32, 33 and 34). It is crucial that the EVN actively engages in both these approaches to push toward the highest possible resolutions.

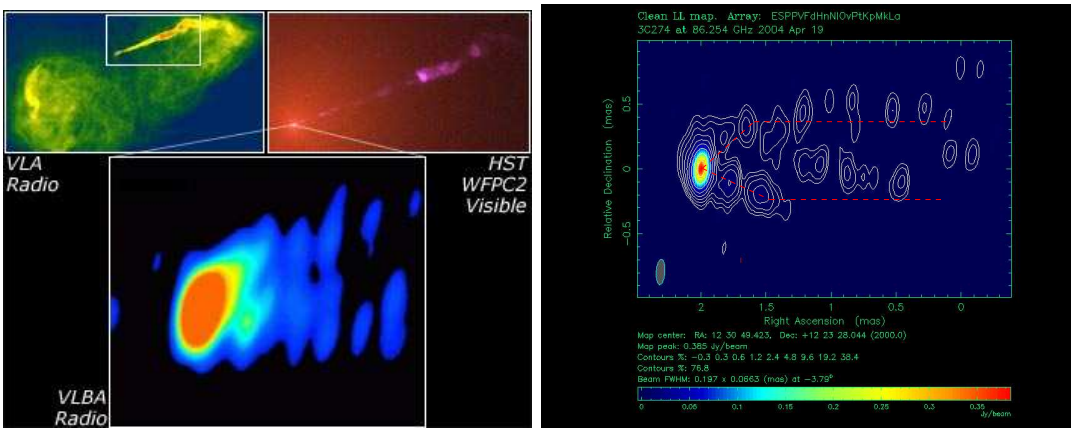

Figure 34: Left: A collage of images of the nearby radio galaxy M87 on a wide range of scales, from those probed by radio observations with the Very Large Array, to those probed by 7mm VLBI. The 7mm VLBI image seems to show limb-brightening and clear evidence for a conical opening of the jet, followed by collimation. Right: A 3mm global VLBI image of M87, which seems to confirm the conical jet opening and collimation shown in the 7mm VLBI image, but makes it possible to study them with higher resolution (Krichbaum et al. 2006).

Owing to the short observing wavelengths involved, mm-VLBI enables studies of compact regions that are self-absorbed, and therefore invisible, at longer cm-wavelengths. The combination of high angular resolution and ability to penetrate through such "opacity barriers" is one of the

biggest strengths of mm-VLBI observations. In addition, global mm-VLBI observations yield the highest absolute resolution attainable with any technique, making it possible to probe sub-parsec scales in AGNs at modest redshifts of $z \geq 0.1$, and even smaller scales of a few milliparsecs (a few light days) in nearby galaxies at Mpc distances ($z \simeq 0.001$). At the same time, it is very difficult to observe some key phenomena with millimetre observations, because their role usually becomes important only at much longer wavelengths; examples include Faraday rotation and the Faraday conversion of linear to circular polarization. These phenomena provide unique *supplementary* information to direct measurements of the total-intensity and polarization of synchrotron radiation. The high-resolution and *long-wavelength* observations provided only by space-VLBI are crucial for AGN studies of fundamental importance.

Present day mm-VLBI observations are done with the VLBA (7mm, 3mm, US-only) and the Global Millimeter VLBI Array (3mm, GMVA). Effelsberg (MPIfR, Germany), Onsala (OSO, Sweden), Metsahövi (MRO, Finland) and the two IRAM telescopes (Pico Veleta, Spain, and Plateau de Bure, France) participate regularly in global 3mm-VLBI sessions, together with the 3-mm VLBA stations. Mainly due to logistical reasons, GMVA sessions occur only twice per year (Spring/Autumn), limiting capabilities for monitoring fast evolution in AGN. Although 43 GHz (7 mm) is formally an EVN frequency, the small number of stations equipped with functional 7mm receivers (at present only Effelsberg, Onsala, and Noto) has limited observing capabilities, leading to infrequent observations at irregular time intervals. Another important factor is that, since mm-VLBI depends on heavy application of amplitude self-calibration (due to the lower atmospheric stability than at centimeter wavelengths), especially mm-VLBI observations benefit greatly from an increased number of participating telescopes.

According to the Ruze formula, $\eta_A \propto \exp -(4\pi\sigma/\lambda)^2)$, the main limitation on an antenna's ability to be used for mm-VLBI comes from the accuracy of the antenna surface σ. For a given observing wavelength λ, the surface rms σ must be smaller than $\lambda/15$ in order to obtain a sufficiently high aperture efficiency. With adaptive optics, this constraint may be somewhat relaxed to $\lambda/10$. Another important aspect is the pointing accuracy, which at a given wavelength should be better than about 1/5 of the beam size (which is $\propto \lambda/D$).

Two currently funded space-VLBI mission are the Russia-led RadioAstron mission, planned for launch in early 2009 and the Japanese-led project VSOP-2, planned for launch in 2015. RadioAstron has operating frequencies at 300 MHz, 1.6, 4.8 and 18.4-25.1 GHz. The frequencies to be included in VSOP-2 are 8, 22 and 43 GHz, with dual-polarization at all frequencies.

17 Unravelling the mysteries of microquasars

Microquasars are Galactic X-ray binaries (Fig. 35) with the ability to generate relativistic jets with bulk Lorentz factors even comparable to those in active galactic nuclei (AGNs). About a decade ago, these objects attracted attention as nearby, smaller-scale accessible laboratories for studying the same accretion and ejection phenomena observed in AGNs on much larger spatial and temporal scales. This interest persists today, and microquasars are beginning to fit into our general understanding of accretion phenomena in the Universe. In particular, we are beginning to quantitatively understand the connection and scaling between the radio and X-ray luminosities generated in jets and accretion disks (see Fender 2006 for a modern review). However, significant problems remain incompletely understood, some revealed by previous VLBI observations. The European VLBI array envisioned in this document will enable more continuous monitoring of microquasars and other stellar sources, thus making it possible to catch phenomena seldom observed with VLBI techniques and with unprecedented sensitivity.

17.1 All microquasars VLBI-accessible and routinely monitored

The anticipated sensitivity (~ 1 μJy beam^{-1} in one hour), frequency agility and rapid response time envisaged to be developed for the EVN over the next decade will be key to (i) put all microquasars within reach of VLBI observations, (ii) boost research in transient studies and (iii) allow high quality polarization imaging at sub-mJy level (including circular polarization).

We know today of about 15 microquasars populating the Milky Way (Paredes 2005), many of which are prime targets for various X-ray, gamma-ray and other ground-based facilities. Thus far, only the brightest (e.g. Cygnus X-3, SS433, Cygnus X-1, GRS 1915+105) have been well studied at radio wavelengths with milli-arcsecond angular resolution. The rest of this population has been hardly observed with VLBI techniques, mainly due to the weakness of their radio emission or their fast time variability (epochs when they are bright often do not coincide with the fixed dates of VLBI sessions). Improved higher sensitivity VLBI observations will allow to routinely extend the VLBI data to fainter radio-emitting X-ray binaries. Directly resolving the jets in these microquasar candidates would provide a significant boost in this field. Increasing the scarce microquasar population currently known will at last enable statistically robust comparisons of system properties, such as testing whether there is an underlying high-Lorentz-factor jet in all microquasars, as is suggested for Cyg X-1. The presence of emission structures nearly perpendicular to the jet direction, as in SS 433, is another interesting issue that could be addressed with very deep VLBI maps. Moreover, the ability to measure sub-mJy polarization also becomes essential for magnetic-field studies and constraining the jet composition.

Figure 35: Schematic of an interacting stellar binary system with matter accreting from one of the stars onto its companion, which may be a compact object (white dwarf, neutron star or black hole). Such interactions give rise to activity from the radio to the X-ray.

17.2 The role of e-EVN in microquasar research

The fast variability of microquasars and X-ray binaries is well adapted to the e-VLBI strategy being developed at JIVE. A significant fraction of e-VLBI proposals submitted during the first 2006–2007 calls were devoted to microquasars, and the first results have recently been published (Tudose et al. 2007, Fig. 36; Rushton et al. 2007). It is foreseen that the EVN will be able to arrange observations of transient sources within 24 hours as early as 2007–2008. With adaptive scheduling, this could be significantly reduced, which is absolutely essential for observing stellar sources that are variable on timescales of hours to days. The envisioned uv-coverage of the EVN will let us produce movies of the source structural evolution from snapshot images made from only a few minutes of data. In addition to responding to an outside trigger, another possible application of e-VLBI is to monitor a group of known transient sources with e-VLBI and alert the community about observed activity, to initiate observations with other instruments. The e-EVN

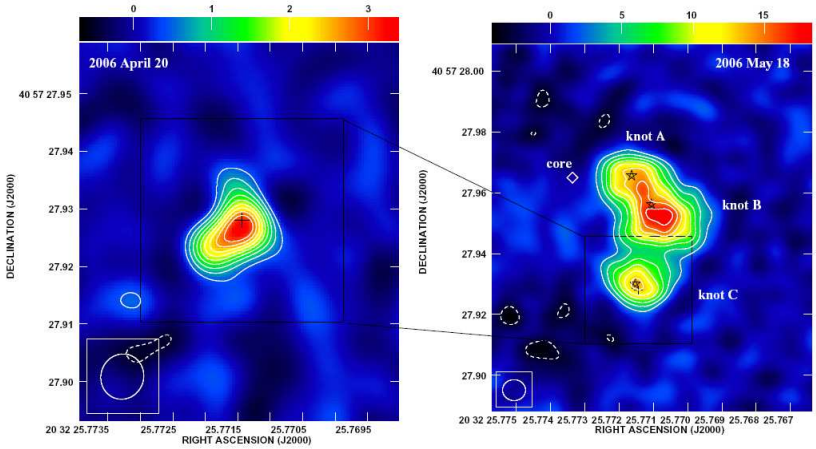

Figure 36: Left: 5 GHz e-VLBI map of Cygnus X-3 on 2006 April 20. Right: 5 GHz e-VLBI map of Cygnus X-3 on 2006 May 18. Note the change between the two images. From Tudose et al. (2007)

science-result turnaround time is already sufficiently short today to carry out such observations.

The EXPReS project has made important steps towards a global e-VLBI array, exercising Internet connections to South America and Australia. If this could be extended further, 24-hour e-VLBI monitoring of microquasars could be done easily. Previous campaigns with continuous VLBI monitoring have led to the discovery of a very high Lorentz-factor, radiatively inefficient, energy flow in the jets of the low-mass microquasar Scorpius X-1 (Fomalont, Geldzahler & Bradshaw 2001). The existence of such dark flows is also known to occur in high-mass systems such as Cygnus X-1 (Gallo et al. 2005), and is one of the unsolved questions in this field.

Continuous monitoring of these sources is also essential to understand how changes in the accretion disk are related to jet-production mechanisms. Is there a difference between outflows in neutron-star and black-hole binaries? Do neutron stars produce outflows with speeds of only ~ 0.3c, while jets from black holes are always highly relativistic? Or does the jet speed in an X-ray binary system change as the X-ray state of the system changes, introducing shocks in the outflow, as is generally thought today? Observations of what is happening to the radio jet when the X-ray state is changing will be a challenging task even for e-VLBI, because there is no known well defined trigger for these events. One possible sign of an imminent change in the X-ray state could be the quenching of the radio emission before/during the accretion disk's state changes. This may be related to a complete depletion or disruption of the radio core and jet, as is indicated by serendipitous observations of a radio flare in SS433 (Fig. 37).

17.3 Gamma-ray binaries

Micro-quasars and X-ray binaries have now also been detected as high-energy (TeV) gamma-ray sources (Aharonian et al. 2005; Albert et al. 2006). Results from the modern generation of Cherenkov telescopes (H.E.S.S., MAGIC, VERITAS, etc.) combined with intensive VLBI observations have opened a completely new field, leading to the idea that there exists a group of "gamma-ray binaries" (Dubus 2006; Mirabel 2006a). This is currently a general concept that could broadly include both micro-quasars and pulsar X-ray binaries. Which of the two physical scenarios is more common is an on-going debate (see Mirabel 2006b). The EVN could play a

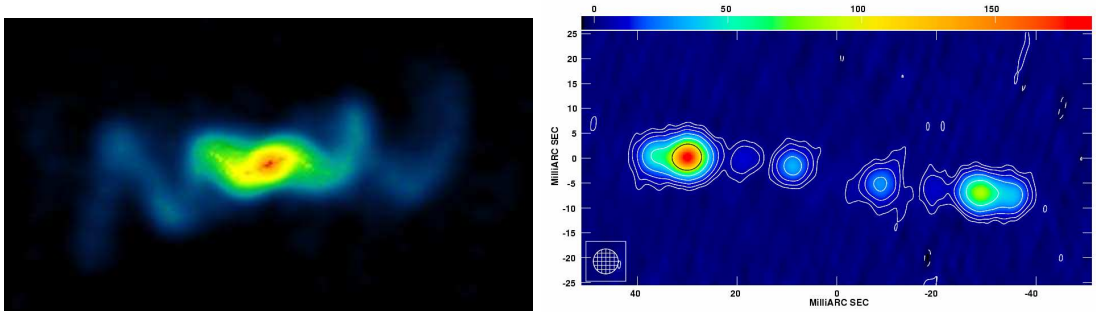

Figure 37: Left: Radio image of SS 433 by the Very Large Array displaying the corkscrew-pattern resulting from the precessing jet. Right: SS 433 during a flare in 1998 as observed by Paragi et al. (1999),showing pairs of components moving outwards from the centre to the East and West, with a velocity of $0.26c$. The core-jet itself faded completely during the event.

crucial role in this exciting field during the coming years, in association with new existing or planned gamma-ray facilities (e.g. GLAST and CTA).

Thus far, both VLBI data and theoretical models of the first gamma-ray micro-quasar – the high-mass system LS5039 – are consistent with a scenario where the TeV gamma-rays are mainly due to inverse Compton scattering of various populations of seed photons scattered by the relativistic electrons in the radio jet (Paredes et al. 2000; Paredes, Bosch–Ramon & Romero 2006). This same mechanism was believed to be at work in the massive X-ray binary LSI+61303. However, recent VLBI observations have revealed that the radio and gamma-ray emission in this source is most likely due to the interaction of a relativistic wind from a young pulsar with the circumstellar envelope of the Be companion star (Dhawan, Mioduszewski & Rupen 2006). The orientation of the radio emitting region in LSI+61303 varies with the orbital phase, supporting the pulsar scenario. In this way, sampling of the full orbital cycle with VLBI observations provides an elegant way to discriminate between various scenarios for gamma-ray binaries on a case by case basis. It is likely that more systems of this kind will be discovered in the future through such observations.

17.4 X-ray binaries, micro-quasars and ultra-luminous X-ray sources in nearby galaxies

The envisioned sensitivity of the EVN will enable for the first time useful observations of X-ray binaries and micro-quasars in nearby galaxies. These sources represent a possible physical framework for understanding the ultra-luminous X-ray sources (ULXs) observed in various types of galaxies. It is believed that geometric beaming of the X-ray and radio emission could be the origin of the apparently high luminosities observed. An alternative model is that some ULXs are associated with accretion onto intermediate mass black holes (IMBHs). Currently, we are not able to place strict limits on the masses of black holes in ULX sources based on VLBI observations. However, this will become possible for ULX's in nearby galaxies using the future enhanced EVN.

18 Stellar powerhouses

18.1 Radio supernovae

Radio emission has been detected from only a small fraction of supernovae (see http://rsd-www.nrl.navy.mil/7214/weiler for a complete list), and only a small fraction of radio supernovae can be studied with the very high-resolution provided by VLBI. Radio emission has never been detected from Type Ia supernova (believed to be the result of an exploding carbon–oxygen white dwarf in a binary system; Woosley, Taam, and Weaver 1986). On the contrary, radio emission has been detected for a number of Type Ib, Ic and II supernovae (believed to be the results of the gravitational collapse of massive stars). Typically, Type II supernovae are more radio luminous than Types Ib and Ic.

Radio supernovae are usually explained within the standard interaction model (SIM), initially proposed by Chevalier (1982). In this model, a strong interaction between the high-velocity expanding supernova ejecta and the ionized circumstellar medium is expected, resulting in the formation of a self-similarly expanding shell-like structure that gives rise to the observed synchrotron radio emission at centimeter wavelengths. The radio brightness of the supernova increases rapidly with time, due to the decreasing optical depth in the line of sight. Once the brightness has reached its maximum, the emission decreases monotonically due to expansion losses. The models have been modified to include thermal and non-thermal absorbers of the radiation, as well as synchrotron self-absorption as an additional absorbing mechanism, to allow alternative power-law profiles for the circumstellar medium, and to include the role of radiative losses in the supernova evolution.

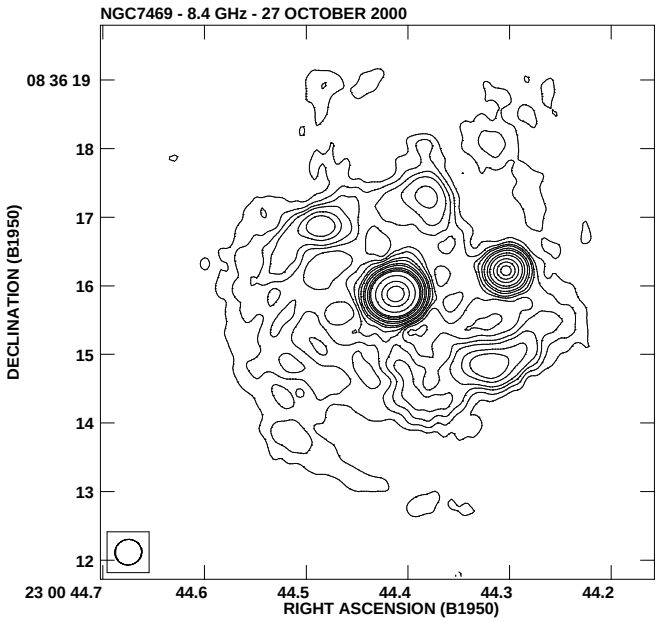

Figure 38: 8.4 GHz VLA A-configuration image of NGC 7469 from observations on 27 October 2000. SN 2000ft is located in the circumnuclear starburst at a distance of 600 pc of the nucleus (Alberdi et al. 2006).

Multi-wavelength radio light curves and VLBI observations of radio supernovae at cm wavelengths are a powerful tool for probing the circumstellar interaction that takes place after a supernova explodes. High-resolution radio observations enable us to trace the pre-supernova mass-loss history through direct imaging of the structure of the supernova as it expands. The wealth of information provided includes direct estimates of the deceleration of the supernova expansion, the density profiles for the ejecta and circumstellar medium (which have implications for the progenitor of the system), distortion of the shock front, the magnetic-field intensities, and the potential observation of Rayleigh–Taylor instabilities.

EVN studies of radio supernovae are currently severely limited by the sensitivity of the array

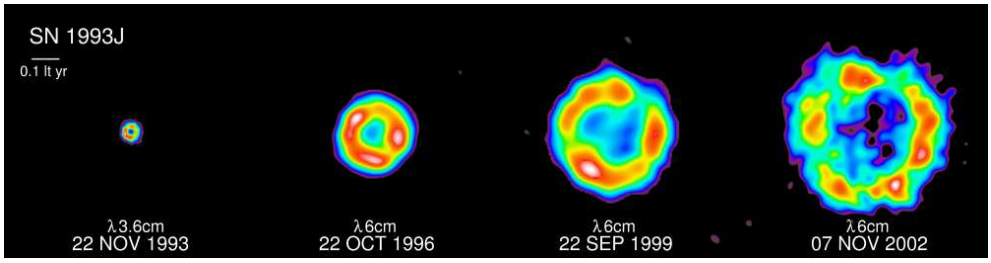

Figure 39: Sequence of images of SN 1993J from VLBI observations obtained 239, 1304, 2369 and 3511 days after explosion (Marcaide, Alberdi & Ros 1995).

(typically, radio supernovae have peak flux densities of only a few mJy). The projected EVN over the coming decade and beyond will have a sensitivity of about 2.5 microJy in 10 min, thus enabling the detection (at the 4σ level) of SN1993J-like events (SN1993J is an average radio supernova) out to distances of 350 Mpc. Scientific goals for future EVN observations of radio supernovae include the following:

(i) Characterizing and studying the supernova structure, shell width and angular expansion of young Type Ib/c and II supernovae. High-sensitivity future EVN observations would make it possible to extend these studies to low luminosity radio supernovae.

(ii) Studying radio supernovae at early ages, close to the epoch of the explosion, during the optically thick phase of the radio light curve, which carries information about the physical processes dominating the absorption (homogeneous and/or clumpy external medium, synchrotron self-absorption, Razin–Tsytovich effect). This could be achieved with the EVN at 5 GHz with a wide bandwidth of 4 GHz, enabling direct and simultaneous acquisition of spectral information. Since the spectral evolution during the rising phase of the light curve changes very rapidly, the ability of the EVN to react to target of opportunity proposals within days would make it possible to uniquely characterize the physical parameters of the circumstellar medium into which the supernova shell is expanding.

(iii) Long-term monitoring of the supernova expansion, investigating the possible existence of various deceleration regimes and verifying whether the expansion is self-similar (e.g., SN1993J (Marcaide, Alberdi & Ros 1995; Fig. 39).

(iv) Through long-term monitoring of the supernova expansion, studying the transition from radio supernova to supernova remnant (i.e., from interaction of the supernova ejecta with the *c*ircumstellar medium to interaction with the *i*nterstellar medium). It is of interest to re-observe "historical" VLBI supernovae (e.g., SN1979C (Marcaide et al. 2002); SN1986J (Pérez–Torres, Alberdi & Mardaide 2002), SN2001gd (Pérez–Torres et al. 2005)), to see how they evolve into supernova remnants.

(v) Searching for compact objects at the centers of supernova explosions, similar to the pulsar found in SN1986J (Bietenholz, Bartel & Rupen 2004).

(vi) Studying the spectral-index evolution of radio supernovae, the spectral-index distribution within the shell structure, and the role of the changing opacity from the part of the shell behind the supernova ejecta in determining the observed size. These tasks require quasi-simultaneous multi-frequency observations of radio supernovae.

(vii) High-sensitivity VLBI polarization observations would make it possible to determine the magnitude and structure of the magnetic field within the shell structure (Is the magnetic field constant, or does it decrease radially from a maximum at the contact discontinuity or at the

forward shock? Is the magnetic field the result of turbulent amplification or of the compression of the circumstellar magnetic field?)

(viii) Detecting or placing much more stringent upper limits on the radio emission from Type Ia supernovae, which have not yet been detected in the radio.

(ix) Detecting low luminosity radio supernovae and studying groups of radio supernovae within a single galaxy at different stages of their evolution, from recently exploded young supernovae (even the initial, inverted-spectrum phase) to supernova remnants, and using this as a tool to probe the interstellar medium in various regions in the galaxy.

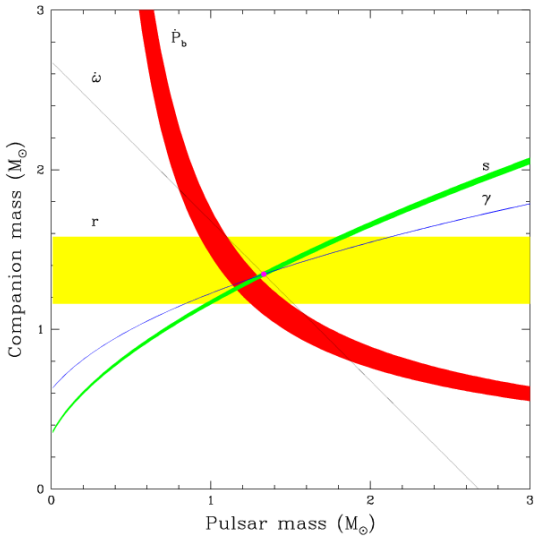

Figure 40: This diagram indicates all constraints on the masses of the two neutron stars in the binary system containing PSR B1534+12. The constraints from the advance of periastron ($\dot{\omega}$), the Shapiro delay (r & s), and the gravitational redshift term all intersect at a single point, as expected in general relativity. The Post-Keplerian parameter ($\dot{P}_b$) corresponding to orbital decay via the emission of gravitational waves does not coincide with the other constraints, possibly due to the poorly determined transverse velocity of the system. High-sensitivity VLBI with pulsar binning will be able to determine the parallax and proper motion independently, making possible tighter constraints for tests of gravity theories.

(x) Searching for radio supernovae in distant Luminous Infrared Galaxies (LIRGs). The current sensitivity limits such high-resolution radio studies to distances of a few hundred Mpc (e.g., SN2000ft in NGC7469; Alberdi et al. 2006; see Fig. 38). With the expected increased sensitivity of the future EVN, it will become possible to detect SN2000ft-like events to distances of at least 1 Gpc, enabling the determination of the supernova rate and its relation to the rate of massive star-formation.

18.2 Radio pulsars and transients

The message for pulsar research with the Square Kilometer Array is: *find them, time them, and VLBI them.* The EVN provides a great scientific and technical platform for the last of these steps. There are three main scientific goals of VLBI observations of radio pulsars: astrometry, pulsar emission and pulsar environments.

Astrometry is a key application of VLBI observations of radio pulsars. Parallaxes and proper motions are essential for determining the space velocities of radio pulsars. While pulsar timing can sometimes provide information about transverse velocities, in most cases, the timing signatures of proper motion and parallax are masked by timing irregularities. The parallax, in particular, is very difficult to measure even for millisecond pulsars, and VLBI provides the best method for determining pulsar distances. Indeed, only simultaneous measurements of proper motion and parallax provide unambiguous and accurate transverse speeds, since the distances derived from the pulsar dispersion measure and some model of the Galactic electron distribution are often highly uncertain. However, improving our understanding of pulsar velocities is crucial for studies of the physics of the asymmetric supernova explosions in which pulsars are formed, and which provide the "kicks" that lead to the large observed space velocities. Moreover, pul-

sar velocities, especially for young populations, enable us to determine their birth locations and whether or not they are associated with supernova remnants.

Combined with accurate pulsar dispersion measures, accurate parallax distances can be used to directly probe the interstellar medium by enabling determination of the electron column density along that line of sight. Even measurements of a relatively small number of parallaxes can provide crucial constraints on the distribution of the interstellar medium near the sun. If the rotation measure of the pulsar is also known, we can begin to unravel the local magnetic-field structure.

Precision timing and gravity - Independent determinations of parallaxes and proper motions using VLBI have important applications for precision pulsar timing as well. In the case of pulsars displaying significant timing noise, constraining the position, parallax and proper motion enables more accurate determination of the nature of the timing noise and the rate at which the pulsar's rotation is slowing. One of the most important applications is using pulsars for precision tests of theories of gravity, for example, determining currently unknown or poorly constrained distances to relativistic binaries and the velocities of these systems (see, for example, Kramer et al. 2004). Here, kinematic effects bias the observed values of some post-Keplerian parameters used to study possible deviations from general relativity. Indeed, the tests of theories of gravity provided by the Hulse–Taylor pulsar or PSR B1534+12 are purely limited by our inability to correct for kinematic effects and/or poorly constrained distances (Fig. 40).

Emission mechanisms - VLBI also has the potential to help in determining or constraining the emission mechanism operating in radio pulsars. In some cases, radio pulsars show emission across the entire pulse period, or from an apparently very wide emission beam. An important test of the underlying beam geometry is whether there is weak emission in between two well separated peaks. VLBI with binning at the pulse period can be used to determine whether these pulsars ever turn off or if there is a DC component to their emission that cannot be detected with standard pulsar data acquisition systems. The information obtained from such studies can then be used to investigate the particle acceleration mechanism itself, if it turns out that we are looking right along the magnetic poles of some of these pulsars. High-sensitivity VLBI observations may also be able to resolve the magnetospheres of the most nearby radio pulsars, giving us a unique insight into this important region.

Environmental effects - VLBI with pulsar binning also provides an excellent tool for studying the interaction of a radio pulsar with its environment. The vast majority of the spin-down energy of a radio pulsar is lost in its relativistic wind, and is only observed when it interacts with the interstellar medium in the form of a pulsar wind nebula. These nebulae are seen throughout the electromagnetic spectrum, but only rarely in the radio, mainly because the radio nebulae are very small and thus difficult to resolve. The high spatial resolution of VLBI combined with binning, which allows us to make "off-pulse" maps, could reveal many more of these nebulae in the radio. Their compact nature means that they reflect emission from the youngest electrons, and so provide a unique probe of the wind and innermost shocks. Combined with observations at other wavelengths, VLBI with binning provides a tool for studying both the wind structure and the interstellar medium. In particular, it may be possible to study the jets and tori seen in the X-rays on much smaller radii.

e-VLBI and transient phenomena - The advent of e-VLBI has opened up new territory for VLBI studies of radio emitting neutron stars. A number of new transient forms have been identified, such as Magnetars, RRATs and Intermittent Pulsars. Flexible VLBI as enabled by e-VLBI makes it possible to determine the fluxes, positions and, eventually, parallaxes and proper motions of these objects before they fade away. The sensitivity provided by the EVN will be key for some aspects of these studies, such as measuring the polarization of the transient emission (e.g. Brocksopp et al. 2007). Precise position information, in particular, is crucial to proper

source identification in various parts of the electromagnetic spectrum.

EVN requirements - All the above studies have two key requirements for future EVN arrays and correlators: increased sensitivity and pulsar binning. The former comes by including more telescopes, but also by increasing the bandwidth which can be transported and correlated. The latter is correlator specific, and requires that it be possible to have at least 64 bins across the pulse profile. Significant frequency resolution is also required, so that corrections for dispersion in the interstellar medium can also be made. Ideally, it should also be possible to specify multiple pulsar binning rates, so that multiple pulsars, such as might be found in globular clusters, can all be analysed simultaneously. The continuation and expansion of e-VLBI will provide additional opportunities to study the rapidly growing class of transient radio emitting neutron stars.

EVN tied-array operation - An exciting but as yet unexplored possibility for the EVN is combining all of the telescopes to form a so-called "tied-array". Interspersing observations of a pulsar with regular observations of strong calibrators should make it possible to sum coherently the signals from EVN telescopes and then output a baseband signal that could be analysed by a coherently de-dispersing pulsar backend. The power of this approach becomes clear when we consider that, with a tied array of nine telescopes with an average size of 64m would have a sensitivity equivalent to a single dish larger than 200m in size. Combined with the very wide bandwidths anticipated for future EVN observations, this tied-array would be the most sensitive pulsar telescope in the world. Not only would it be a great technical step on the road to the Square Kilometer Array, which also faces challenges such as forming tied-arrays, but it would also be a fantastic new scientific tool. It would enable us to achieve unprecedented sensitivities for high precision timing, and possibly even to time pulsars with sufficient precision to be able to detect gravitational waves from the early Universe.

References to Chapter D

Alberdi A., Colina L., Torrelles J.M. et al. 2006, ApJ 638, 938

Bietenholz M.F., Bartel N. & Rupen M.P. 2004, Sci 304, 1947

Brocksopp C., Miller–Jones J.C.A., Fender R.P. & Stappers B.W. 2007, MNRAS, 378, 1111

Casse F. & Keppens R. 2004, ApJ, 601, 90

Chevalier R.A. 1982, ApJ 258, 790

Croke S.M., Gabuzda D.C. & Katz D. 2008, MNRAS, in preparation

Dhawan V., Mioduszewski A.M. & Rupen M. 2006, VI Microquasar Workshop, Proceeding of Science, `http://pos.sissa.it//archive/conferences/033/052/MQW6_052.pdf`

Dubus G. 2006, A&A, 456, 801

Fender R.P. 2006, in *Compact Stellar X-ray Sources*, Cambridge Astrophysics No. 39, 381

Fomalont E.B., Geldzahler B.J. & Bradshaw C.F. 2001, ApJ, 553, L27

Gabuzda D.C. 1999, New Astron. Rev., 43, 691

Gabuzda D.C. 2000, in Astrophysical Phenomena Revealed by Space VLBI, ISAS, Tokyo, p. 121

Gabuzda, D.C. 2007, Proc. 8th EVN Symp., www.astro.uni.torun.pl/evn2006/index.php

Gabuzda, D.C., Vitrishchak V.M., Mahmud M. & O'Sullivan S.P. 2008, MNRAS, submitted

Gallo E., Fender R., Kaiser C., et al. 2005, Nature, 436, 819

Kramer M., Backer D.C., Cordes J.M., Lazio T.J.W., Stappers B.W. & Johnston S. 2004, New Astron. Rev., 48, 993

Krichbaum T.P. 2007, Proc. 8th EVN Symp., www.astro.uni.torun.pl/evn2006/index.php

Krichbaum T.P., Graham D. A., Bremer M., Alef W., Witzel A., Zensus J. A. & Eckart A 2006, Journal of Physics: Conference Series, Volume 54, Issue 1, pp. 328; arXiv:astro-ph/0607072

Lobanov A.P. 1998, A&A Suppl, 132, 261
Lobanov A.P., Krichbaum T.P., Witzel A., Kraus A., Zensus J.A., Britzen S., Otterbein K., Hummel C.A. & Johnston K. 1998, A&A, 340, 60L
Maccarone T. 2004, MNRAS, 351, 1049
Marcaide J.M., Alberdi A, Ros E. et al. 1995, Sci 270, 1475
Marcaide J.M., Pérez–Torres M.A., Ros E. et al. 2002, A&A 384, 408
Mirabel 2006a, arXiv:astro-ph/0610707
Mirabel 2006b, Science, 312, 1759
Paragi Z. et al. 1999, New Astron Rev. 43, 553
Paredes J.M., Martí J., Ribó M., et al. 2000, Science, 288, 2340
Paredes J.M. 2005, Chinese Journal of Astronomy and Astrophysics, 5, 121
Paredes J.M., Bosch–Ramon V. & Romero G.E., 2006, A&A, 451, 259
Pérez–Torres M., Alberdi A. & Marcaide J.M. 2002, A&A 394, 71
Pérez–Torres M., Alberdi A., Marcaide J.M. et al. 2005, MNRAS 360, 1055
Rushton A., Spencer R.E., Strong M. et al., 2007, MNRAS, 374, L47
Tudose V., Fender R.P., Garrett M.A., et al. 2007, MNRAS, 375, L11
Woosley S.E., Taam R.E. & Weaver T.A. 1986, ApJ 301, 601

Technical Requirements

19 EVN system sensitivity

The inclusion of new telescopes and significantly wider bandwidths will provide a step-change in sensitivity for continuum studies. Bandwidths of 250 MHz (data rate of 1 Gb/s) at L-band and 1 GHz at C-band (data rate of 4 Gb/s) and above is achievable with today's technology. This would allow sub-μJy continuum sensitivities with a full imaging run. Continuum and spectral line studies would benefit from further improvements of current receiver systems utilizing the latest technological advances. This is particularly true for the high-end of the spectral range of 43 GHz and above. The back-end systems must be upgraded to allow for data rates exceeding 4 Gb/s, with digital IFs that could be easily configured for narrow band spectral observations, but could accommodate broad IFs as well, for observations of broad (> 1000 km/s) spectral lines.

Half of the science topics in the previous chapters stress the importance of seamless integration of e-MERLIN telescopes into EVN2015 (see Table 2). This would boost the sensitivity as well as improve on the short-spacing coverage. EVN telescopes could also be added to the e-MERLIN correlator. Spectral index imaging would greatly benefit from these developments, because matching resolutions at different frequencies could be easily achieved with different array configurations.

20 Frequency coverage and agility

There is a need to equip all telescopes (where possible) with broad-band, dual polarization receivers at GHz frequencies. The X-band receiver update will be crucial for EVN ground support of the VSOP-2 project (Sect. 16.2). New state of the art (MMIC, HEMT) receivers at 22 GHz, 43 GHz and above would allow the study of the most inner parts of AGN, and would provide resolution-matched EVN2015 images to complement VSOP-2 data. Multi-frequency systems (i.e. 22/43/86 GHz) could be considered as well. This would allow frequency phase-referencing with correction of atmospheric phase variations at the correlator, and would provide simultaneous ground VLBI data accompanying VSOP-2 observations. The highest frequencies require high quality antenna surfaces and good pointing capability. In addition, there is an interest to expand the frequency coverage to well below 1 GHz (down to 300 MHz), for continuum gravitational lens studies (Sect. 7), and for redshifted HI and OH spectral lines observations (Sect. 10.3). Methanol maser studies of collapsing gas clouds at stellar birthplaces (Sect. 13.1) would require receivers in the $12 - 15$ GHz range, while at 30 GHz there could be common frequency coverage between EVN2015 and ALMA. The majority of the EVN2015 science topics demands frequency agility with rapid frequency switching times shorter than a minute (see Table 2).

Polarization purity is also on the top of the demand list. The polarization leakage must not exceed 5% for the provision of integrated polarizations for polarization-angle calibrator sources and/or instrumental values for polarization-angle calibration. Westerbork synthesis array data on calibrators must be made available in the EVN archive for optimal gain and polarization calibration. For bands where the WSRT cannot observe, an alternative solution is necessary.

21 Resolution, spacings and field of view

The increased sensitivity places stringent requirements on the dynamic range achievable with EVN2015. Improved imaging fidelity is crucial for all science topics covered in this document.

This is an issue related to network expansion, wider frequency coverage and improved calibration as well as data processing methods. New telescopes in strategic places (e.g. North Africa, Eastern Europe and Asia) are required. Broad-band observations using multi-frequency synthesis will provide excellent maps even in snapshot observing mode. The latter is important for VLBI surveys as well as observations of Galactic transients (Sect. 18.2).

The addition of new Chinese telescopes, including the 500-m FAST, and MeerKAT in South Africa would be highly beneficial for studying compact sources. e-MERLIN integration on the other hand would greatly improve the brightness temperature sensitivity of the array. This would be important for: 1) the increasing resolving out of line and continuum emission by VLBI baselines, 2) types of line and extended continuum emission regions, 2) distant and faint sources, such as in a census of OH/IR morphologies close to the Galactic Centre, 3) maser processes, beaming angles, and other physical properties of masering clumps, and 4) polarization structures over a large field. Note that if e-MERLIN telescopes could be individually connected to the EVN correlator, the EVN2015 would be a unique instrument to observe sources bearing milli-arcsecond to arcsecond-scale morphology with excellent fidelity.

The effective primary beam is about 32 m for the non-homogeneous EVN array with a mixture of 75, 40, 32 and 25-m dishes with slightly more smaller dishes (Strom 2004). Various applications would benefit from the full imaging of the effective primary beam, such as simultaneous imaging of nearby starburst galaxies and their companion galaxies (Sect. 6), and observing gravitational lenses (Sect. 7). But in general, large field of view phase-reference imaging of faint targets would benefit from the availability of nearby, in-beam calibration sources. This will place strong requirements on the correlator as well as on the post-processing software and hardware.

22 Correlator considerations

The correlator characteristics are driven by continuum bandwidth, sub-second integrations (required by wide-field imaging), and by the spectral line resolution requirements. For example, bright sources could be observed in sub-kHz channels in the maser ground states to measure precise Zeeman and non-para-magnetic Zeeman splitting and linear polarization. Simultaneous spectral and spatial imaging with multi-frequency synthesis capability will facilitate calibration of complex fields with both spectral line and continuum emission. Co-propagation and Faraday rotation investigations make it desirable to observe as many lines (such as for methanol) as is feasible simultaneously or contemporaneously. Simultaneous observations of two or more transitions of a molecule has many applications.

Desired observing spectral line practices require sub-bands in different configurations and with different widths. Observations with up to 2 GHz at 5 GHz in up to 8 sub-bands, would require 1 MHz in 1 kHz channels and 7250 MHz in 0.5 MHz channels, or some other narrow-wide combination. At 22 GHz, 256 MHz bandwidth would give 3000 km/s in 0.1 km/s channels in dual polarization. Non-contiguous frequency windows covering the instantaneous bandwidth of the receiver allow multi-line observations such as the four transitions of OH at 1.6 GHz.

A future correlator with 256 Gb/s/telescope with 16384 channels per correlation product (for each of LL, RR, LR, and RL) would give 1 kHz channels across 16 MHz; the corresponding velocity resolution at various frequencies is shown in Table 1.

23 Flexible scheduling, rapid-response science

The EVN2015 science case presents strong requirements for a much more flexible array (see Table 2.). This includes extended observing sessions for monitoring programs, coordinated observations

Table 1: Spanned velocity range and spectral resolution for 16384 spectral channels at various frequencies, for 16 MHz and 1 MHz subbands

Frequency	Velocity range 16 MHz [km/s]	Spectral resolution 16384 channels [m/s]	Velocity range 1 MHz [km/s]	Spectral resolution 16384 channels [m/s]
1.4 GHz	3000	183	188	11.5
1.6 GHz	2700	165	169	10.3
4.7 GHz	920	56	58	3.5
6.0 GHz	720	44	45	2.7
6.6 GHz	650	40	41	2.5
12 GHz	360	22	23	1.4
22 GHz	190	12	12	0.7
43 GHz	100	6	6	0.4

with other arrays (in the radio as well as other parts of the spectrum), and, in some cases rapid response science with dynamic scheduling of the array. Long-term monitoring programs are required for e.g. water maser proper motions at weekly intervals (Sect. 14.2), and for following up novae and supernovae (Sect. 18.1). Rapid response to external triggers is required for Galactic transients (Sect. 18.2) and GRBs. Another example is to observe the stellar maximum of semi-regular stars, which may only be known a few weeks in advance (Sect. 14). Rapid response observations might be best carried out using the e-VLBI technique. This would be important from the reliability point of view, but would also open the possibility of planning future observations based on the results of the first epoch. An extreme example of this would be changing the observing schedule dynamically during the observations, in response to early results from the VLBI run, or to parallel flux density monitoring of a sample of rapidly variable stellar sources. Continuous 24-hour global monitoring of some of these objects (e.g. microquasars) would be desirable.

24 Calibration: amplitudes, phase stability & referencing

The gaincurves of the telescopes must be regularly updated. This is particularly important for the EVN, because in some observatories the receivers may change from session to session. More regular system temperature measurements are essential for the highest quality gain calibration, required e.g. for the detection of circular polarization (Sect. 16). For improving the amplitude scale, as well as for calibrating the linear polarization (see above), regular single dish or WSRT monitoring observations of calibrators are necessary.

A number of observing procedures require the transfer of phase, bandpass and amplitude solutions from one sub-band in one configuration to another sub-band in a different configuration. EVN spectral-line phase-referencing may be improved with simultaneous wide-band continuum for the phase-reference source and narrow-band spectral line observations. Wide-band observations with e.g. 8 sub-bands for combined line and continuum modes or configuration switches between scans need to be implemented. Offsets between different configurations or sub-bands can be calibrated in a comparable fashion if the offset is stable for considerable time.

25 Streamlining observing procedures and User Tools

Calibration procedures with fringe finders, phase referencing, amplitude calibrators, bandpass calibrators and polarization angle calibrators take up at least 30% extra observing time per experiment and up to ∼70% for narrow-band spectral line observations. Considering the variability of calibration sources, very long single/scattered observations will not increase useful sensitivity. Streamlined procedures are required.

Analysis tools to remove RFI and suppression algorithms in the acquisition system would be good for polluted spectral bands. This is most important at low-frequencies, where the difficulties of wide-field calibration must be addressed as well. The availability of standard calibration procedures is helpful to the users not only as black boxes within a virtual observatory system but also as modifiable libraries included in special-purpose analysis software.

26 The EVN2015 requirements matrix

The technical requirements for a list of representative science topics are summarized here in Table 2. Most of these will benefit from the increased sensitivity, an increasing number of telescopes, and improved uv-coverage, and these parameters are not listed separately. The other technical requirements drawn from the Science Cases are listed in the following order.

1. Key frequency bands. This indicates whether continuum or line processing is required, and lists the most relevant molecules of interest, as well as if there are special requirements for bands below 1 GHz or higher than 22 GHz.

2. Indicates whether frequency agility would be essential for the field.

3. Wide-field of view observing mode and processing is required.

4. Improved polarization purity is essential.

5. In this column various calibration issues mentioned in the chapters are listed, that will require improved data calibration tools: low-frequency calibration, RFI mitigation, ionospheric and/or tropospheric phase error correction, high-frequency phase-referencing (sometimes in between frequency bands) and improved calibration of circular polarization.

6. e-MERLIN integration would be highly beneficial.

7. High scheduling flexibility is required: extended monitoring observations, coordinated VLBI observations with other telescopes, Target of Opportunity requests, and sometimes immediate feedback (e-VLBI).

8. Other requirements that did not fit into the previous categories, for example high precision astrometry, or building new receivers (12-15 GHz, 30 GHz and higher frequencies).

The rest frame line frequencies of the listed molecules are the following:

CO	carbon monoxide	115.271 GHz (redshifted CO for z>1.67 falls in 43 GHz band)
CH_3OH	methanol	6668.519 MHz, 12.178 GHz, 23.121 GHz, 25.124 GHz, 44.069 GHz
HI	neutral hydrogen	1420.406 MHz
H_2O	water	22.235 GHz
H_2CO	formaldehyde	4829.660 MHz, 14.488 GHz
H_2COH^+	protonated formaldehyde	31.914 GHz, 36.300 GHz
HCN	hydrogen cyanide	88.630 GHz
HCO^+	formylium	89.189 GHz
HNC	hydroisocyanic acid	90.663 GHz
OH	hydroxyl radical	1612.231 MHz, 1665.402 MHz, 1667.359 MHz, 1720.530 MHz, 4660.42 MHz, 4765.562 MHz, 6030.747 MHz, 6035.092 MHz
SiO	silicon monoxide	42.519 GHz, 42.821 GHz, 43.122 GHz, 86.243 GHz, 86.847 GHz

Table 2: The EVN2015 requirements matrix

Subject (SciCase & section)	Key frequency bands	Freq. agility	Wide FOV	Polari-zation	Calibration issues	e-MER LIN	Flex., e-EVN	Other requirements
History of star-formation (A - 5)	GHz cont.							
AGN-Starburst connection (A - 6)	GHz cont.		√					
Gravitational lenses (A - 7)	GHz cont., $\ll 1$ GHz		√		low-freq cal., RFI	√	√	modifiable libraries for data processing
Low-luminosity AGN (B - 8)	GHz cont.	√		√	circular polarization		√	
Radio hot spot evolution (B - 8.3)	GHz cont.	√	√	√		√		
Extreme star formation (B - 9)	GHz cont., HI line	√	√	√		√		
ISM components in AGN (B - 10)	cont.; HI, OH $\ll 1$ GHz		√		low-freq cal tools			
Megamasers (B - 10.2)	OH, H_2CO H_2O			√		√		
The birth of stars and planets (C - 13)	cont.; CH_3OH OH, H_2CO, H_2O	√	√	√		√	√	$12-15$ GHz; 30 GHz for ALMA!
Search for nearby planets (C - 13.1)	GHz cont.				ion./trop. corrections		√	microarcsec astrometry
Molecules and dust from cool stars (C - 14.1)	OH, SiO, H_2O $22-43$ GHz!	√			high-freq phase-ref			microarcsec astrometry
Maser physics (C - 14.2)	H_2O, H_2CO, OH, H_2COH^+			√		√		
Low-mass binary evolution (C - 14.3.1)	GHz cont.	√		√		√	√	
WR stars and their progenitors (C - 14.3.2)	GHz cont.	√				√	√	coordinated VLBI, optical/IR obs.
Solar System science (C - 15)	GHz cont. S/X				ion./trop. corrections		√	high-precision astrometry
Physics of relativistic jets (D - 16)	GHz cont. up to 43 GHz	√		√	circular polarization		√	frequent monitoring obs.
Jets and the nuclear regions of AGN (D - 16.1)	GHz cont. up to 43 GHz	√		√			√	coordinated radio, optical, X-ray obs.
Atomic and molecular material in AGN (D - 16.1.3)	HI, CO OH, HCO^+			√			√	
AGN on sub-parsec scales (D - 16.2)	43, 86 GHz and higher	√		√	mm p-ref trop. corr.		√	adaptive antennas, new receivers
Microquasars (D - 17)	GHz cont.	√		√	circular polarization	√	√	continuous 24-h global monitoring
Local Group XRBs, ULXs (D - 17.4)	GHz cont.		√			√	√	
Radio supernovae (D - 18.1)	GHz cont.	√		√		√	√	long-term monitoring
Pulsars, neutron star transients (D - 18.2)	GHz cont.	√		√	multiple pulsar binning rates		√	astrometry; tied array EVN

This page intentionally left blank

Recommendations to the EVN Board

The technical objectives of the EVN2015 can only be achieved if each of the existing observatories achieves broad-banding its backend and receiver systems, improves frequency agility, introduces digital backend technology and achieves high-speed network access. In the following the most important necessary steps are summarized.

27 Enhancing EVN capabilities

1. Immediate action is needed to extend the IF bandwidth limitations at the telescopes to accommodate bandwidths of at least 1 GHz. The IFs must use digital base-band converters (dBBC), with 8-bit sampling (if feasible) and RFI mitigation. Recording systems capable of handling up to 256 Gb/s should be introduced in the coming years. The goal of recording at this high data rate may turn out to be unrealistic. However, in the coming years the next Ethernet standard capable of 100 Gbps will be introduced. This means that e-VLBI could soon approach the required EVN2015 data rates. We suggest to set up a working group to investigate and initiate these possibilities as soon as possible.

2. The current frequency coverage of the EVN ranges from UHF to 43 GHz with selected numbers of systems and with a most elaborate system between 1.4 GHz and 8 GHz. Expansion of EVN system capabilities is sought below 1 GHz, at 6 GHz, 12–15 GHz, 22 GHz, 30 GHz, 43 GHz and 86 GHz. Frequencies $\geq$ 43 GHz represent the frontier of VLBI research, which will remain unique even in the SKA era.

3. The advent of LOFAR calls for an optimized EVN with high surface-brightness sensitivity at frequencies below 1 GHz, where the resolution is better adapted to map extended structures.

4. New broad-band dual-polarization receivers are required at cm wavelengths, up to 1 GHz bandwidth in C-band and higher. Frequency agility is required between at least a sub-set of important continuum bands, e.g. L, C/X, and K-band. Issues on polarization purity need to be addressed in the short term.

5. Additional telescopes will greatly improve the EVN2015 sensitivity. It is desired that these apply the same backend/recording technology and have the same frequency coverage (as much as possible) and improvements as the rest of the array.

28 Objectives for e-VLBI

6. The EVN has a world-wide leading role in the development and the science applications of the e-VLBI technique. Data rates approaching 1 Gb/s are possible already, and the current limitations are the data acquisition system and the networking equipment. Multiple Gb/s connection of the telescopes to the correlator would allow very high-sensitivity and robust real-time operations for extended times, without disk space limitations at the stations. This is especially required for transient science research, which is expected to be boosted with the advent of SKA-pathfinders and SKA. e-VLBI techniques will also facilitate 24-hour coverage by multi-network VLBI observations.

7. Seamless EVN-MERLIN integration as the shorter baseline core of EVN operations can be achieved with a 32 Gbps connection from one EVN telescope into the e-MERLIN system and multiple Gbps connections of e-MERLIN telescopes into the current EVN correlator at JIVE. This is achievable with existing technology.

29 EVN correlation

8. A new generation EVN correlator at JIVE needs to be built with a capability of up to 256 Gb/s per radio telescope for routine network operation with 32 station capacity to accommodate all network related stations. The requirements also accommodate very high spectral resolution as well as time resolution experiments

9. Further opportunities need to be explored for tracking and calibration of spacecrafts in support of space science related activities.

30 User services and capabilities

10. The calibration and data reduction routines for the non-homogeneous EVN array is more complex. The development of software tools are essential for new and improved data products, advanced data reduction pipelines, Grid applications, and Virtual Observatory applications. In particular, the user community would benefit from improved astrometry, improved phase-referencing procedures, and improved high- and low-frequency calibration procedures.

11. EVN needs to continue to support and enlarge the user community by means of teaching networks, workshops, and symposia, as well as public relations activities. With improved data calibration pipeline and VO capabilities for the EVN archive, it will be possible to attract more users from outside of VLBI institutes. Initiating collaboration with EU universities and especially with EU-led space missions would help broaden the science applications of EVN2015.

12. EVN should seek to continue a certain fraction of over-subscription in order to assure that the best science is being done and a wide range of topics is covered. The Program Committee should continue to be composed of a broad representation of research interests. Improved/simplified procedures may be necessary to deal with an increasing number of triggered and Target of Opportunity projects.

31 EVN Operations

13. More frequent EVN sessions are required in support of monitoring programs. The EVN should be more flexible toward projects that require coordinated observations with other instruments, and should accommodate rapid response science runs with the possibility of immediate feedback, if required.

14. The large EVN collecting area and its geographic location are important factors for the role of the EVN as a very-long-baseline component of the Square Kilometre Array. The EVN needs to develop optimal complementarity for the SKA. The EVN should serve as a technology testbed for SKA.

15. RFI is increasingly a limiting factor for the data quality for EVN and single dish operations. A high priority for spectrum management at all EVN stations and for further development of RFI mitigation techniques is essential.

16. The EVN2015 should ultimately aim for developing a real-time VLBI network on global scales.